Transient Study of Turbulent Flow and Particle Transport in Continuous Slab Casters Using LES

Quan Yuan

Ph.D. Candidate

Department of Mechanical & Industrial Engineering

University of Illinois at Urbana-Champaign

May 10th, 2004

Acknowledgements

- Professor B.G.Thomas & Professor S.P. Vanka
- Accumold
- Algoma Steel Inc.
- Institutet for Metallforskning
- LWB Refractories Company
- Nippon Steel
- Nucor Steel Decatur LLC
- Postech
- FLUENT Inc. (for Providing Software)
- Former CCC Members
- National Science Foundation (DMI-98-00274 and DMI-01-15486)
- National Center for Supercomputing Applications

Objectives

- Develop and validate efficient computational models for computing time-dependent flow and particle transport / entrapment during continuous casting
- Simulate time-dependent turbulent flow in nozzle and mold regions of water models and actual continuous steel casters
- Simulate transport and entrapment of impurity particles during continuous steel casting
- Investigate particle distribution in steel slabs

Outline

- Description of Computational Model
- Results:

(i) Validation of flow velocity simulation in a 0.4-scale water model

(ii) Validation of Lagarangian particle transport simulation in a full-scale water model

(iii) Simulation of liquid-phase velocities in an actual thin-slab steel caster and its corresponding water model

(iv) Simulation of particle transport and capture in an actual thin-slab steel caster

- Conclusions

Continuous Casting Process

Schematic of continuous casting tundish, SEN, and mold

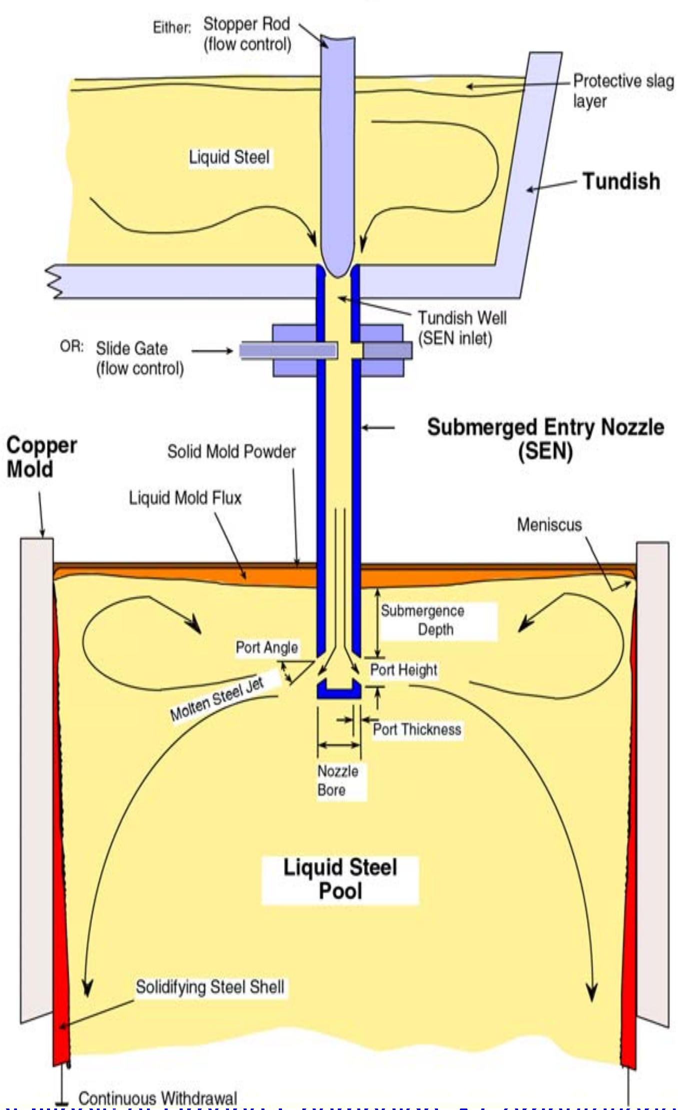

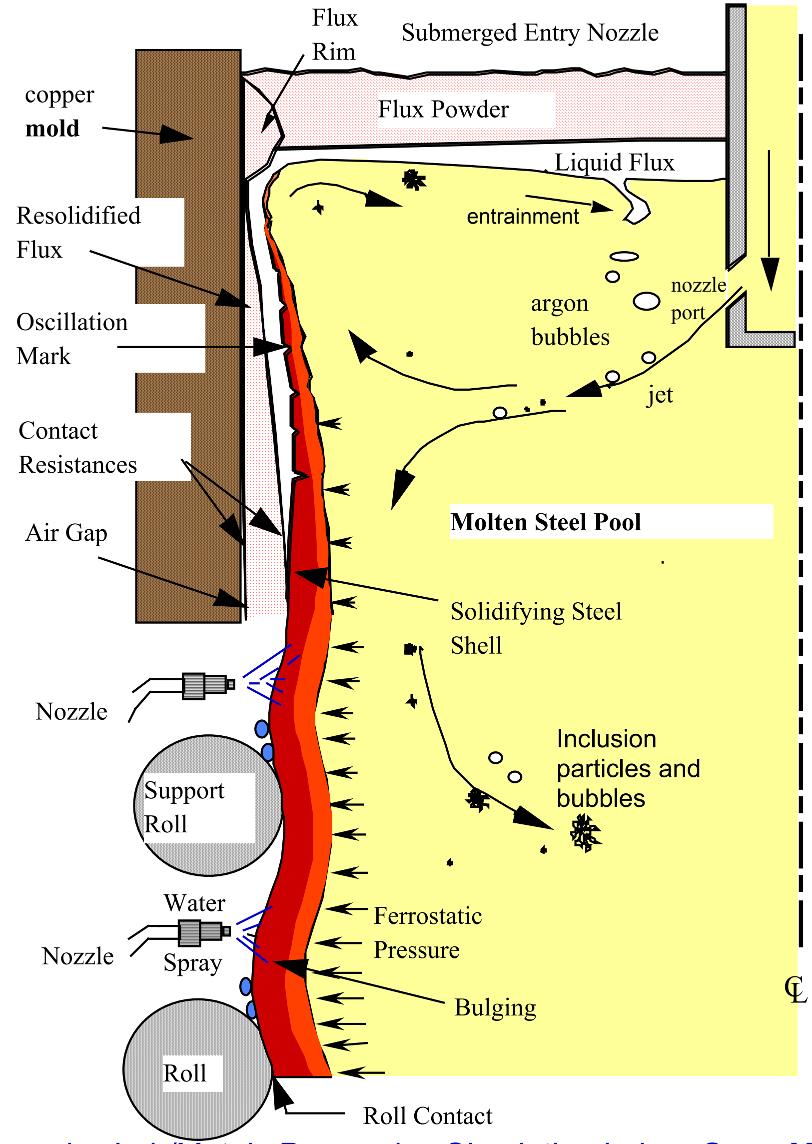

Previous Work

- RANS (Reynolds Averaged Navier-Stokes) of multiphase flow in nozzle and mold region

D. Creech, "Computational modeling of mutliphase turbulent fluid flow and heat transfer in the continous slab casting mold ", M.S. Thesis, Depart. of Mechanical Engineering, UIUC, 1999.

H. Bai, "Argon Bubble Behavior in Slide-Gate Tundish Nozzles during Continuous Casting of Steel Slabs",Ph.D. Thesis, Depart. of Mechanical Engineering, UIUC, 2000.

T. Shi, "Effect of Argon Injection on Fluid Flow and Heat Transfer in Continuous Casting Mold",M.S. Thesis, Depart. of Mechanical Engineering, UIUC, 2001.

- LES (Large Eddy Simulations) of single-phase flow in water models

S. Sivaramakrishnan, "Transient Fluid Flow in the Mold and Heat Transfer Through the Molten Slag Layer in Continuous Casting of Steel",M.S. Thesis,Depart. of Mechanical Engineering, UIUC, 2000.

- Computations on particle motion and capture in continuous casting

R.C. Sussman, M. Burns, X. Huang and B.G. Thomas: "Inclusion Particle Behavior in a Continuous Slab Casting Mold", in 10th Process Technology Conference Proc., Vol. 10, Iron and Steel Society, Warrendale, PA, 1992, pp.291-304.

Governing Equations for Turbulent Flow

Liquid phase (3D time-dependent Navier-Stokes Equations):

- Continuity $$\frac{\partial v_i}{\partial x_i} = 0$$
- Momentum $$\frac{Dv_i}{Dt} = -\frac{1}{\rho}\frac{\partial p}{\partial x_i} + \frac{\partial}{\partial x_j}\nu_{eff}\left(\frac{\partial v_i}{\partial x_j} + \frac{\partial v_j}{\partial x_i}\right)$$

where: $$\nu_{eff} = \nu_0 + \nu_t$$

Used in preliminary simulations of this work

No SGS model LES: $\nu_t = 0$

Smagorinsky SGS Model: $\nu_t = l^2\sqrt{2S_{ij}S_{ij}}$ (J. Smagorinsky,1963)

$$l = \underbrace{C_s}_{0.1}\underbrace{\left(\Delta_x\Delta_y\Delta_z\right)^{1/3}}_{\text{Grid size}}$$ (no wall function)

SGS kinetic energy (k) Model: $$\frac{\partial k_{sgs}}{\partial t} + v_i\frac{\partial k_{sgs}}{\partial x_i} = \nu_t\left|\widetilde{S}\right|^2 - C_\varepsilon\frac{k_{sgs}^{3/2}}{\Delta} + \frac{\partial}{\partial x_i}\left(\nu_{eff}\frac{\partial k_{sgs}}{\partial x_i}\right)$$

where: $\left|\widetilde{S}\right| = \sqrt{2\widetilde{S}_{ij}\widetilde{S}_{ij}}$ $\quad \widetilde{S}_{ij} = \frac{1}{2}\left(\frac{\partial v_i}{\partial x_j} + \frac{\partial v_j}{\partial x_i}\right)$ (K. Horiuti, 1985)

Governing Equations for Particle Transport

Discrete Phase - Particles (Lagrangian Approach):

- Motion $$\mathbf{v}_p = \frac{d\mathbf{x}_p}{dt}$$

- Momentum

$$\frac{d\mathbf{v}_p}{dt} = \underbrace{\frac{18\rho\nu_0}{\rho_p d_p^{\,2}}\left(1+0.15\,\mathrm{Re}_p^{\,0.687}\right)\left(\mathbf{v}-\mathbf{v}_p\right)}_{\textbf{Drag}} + \underbrace{\left(1-\frac{\rho}{\rho_p}\right)\mathbf{g}}_{\textbf{Buoyancy}} + \underbrace{3.07\frac{(\mu_0\rho)^{1/2}}{\rho_p d_p}\left|\boldsymbol{\omega}\right|^{1/2}\left[\left(\mathbf{v}-\mathbf{v}_p\right)\times\boldsymbol{\omega}\right]}_{\textbf{Saffman Lift}}$$

(Spherical inclusion assumption)

where: $\boldsymbol{\omega} = \nabla\times\mathbf{v}$

Details of Numerical Method

- 2^{nd} – Order accuracy in space and time for flow simulations
- Unstructured Cartesian grid and realistic computational domain geometry
- FFT or AMG (Algebraic Multi-Grid) fast solver for pressure Poisson equation
- 4^{th} – Order Runge-Kutta method for particle transport
- One-way coupling and no particle interaction due to low volume fraction of particle phase

Validation of Flow Velocity Computation in a 0.4-Scale Water Model

The 0.4-Scale Water Model

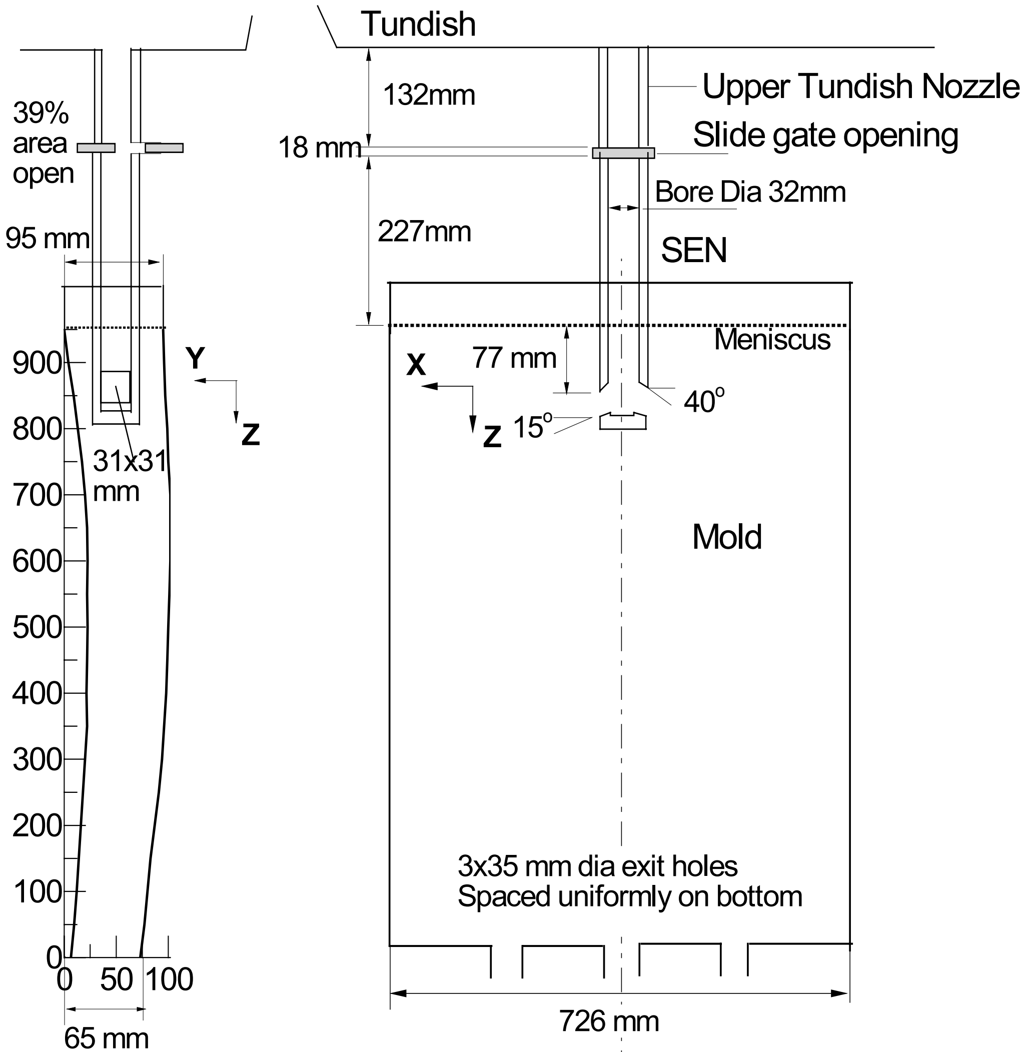

0.4-scale water model at former LTV Steel

Computational domain
(1.6M Cells)

Instantaneous Velocities in Nozzle Region

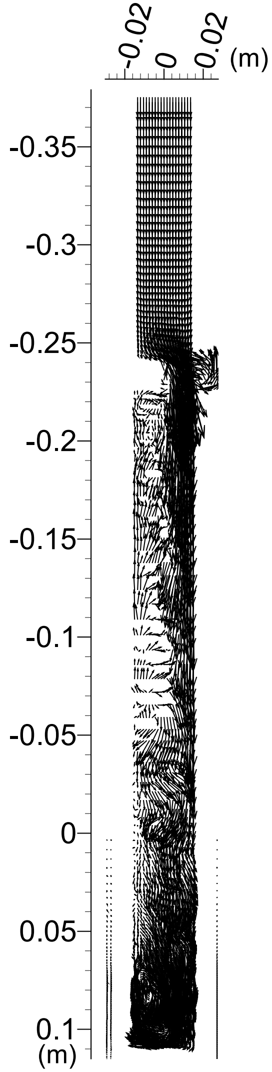

(LES)

Flow at center plane x=0

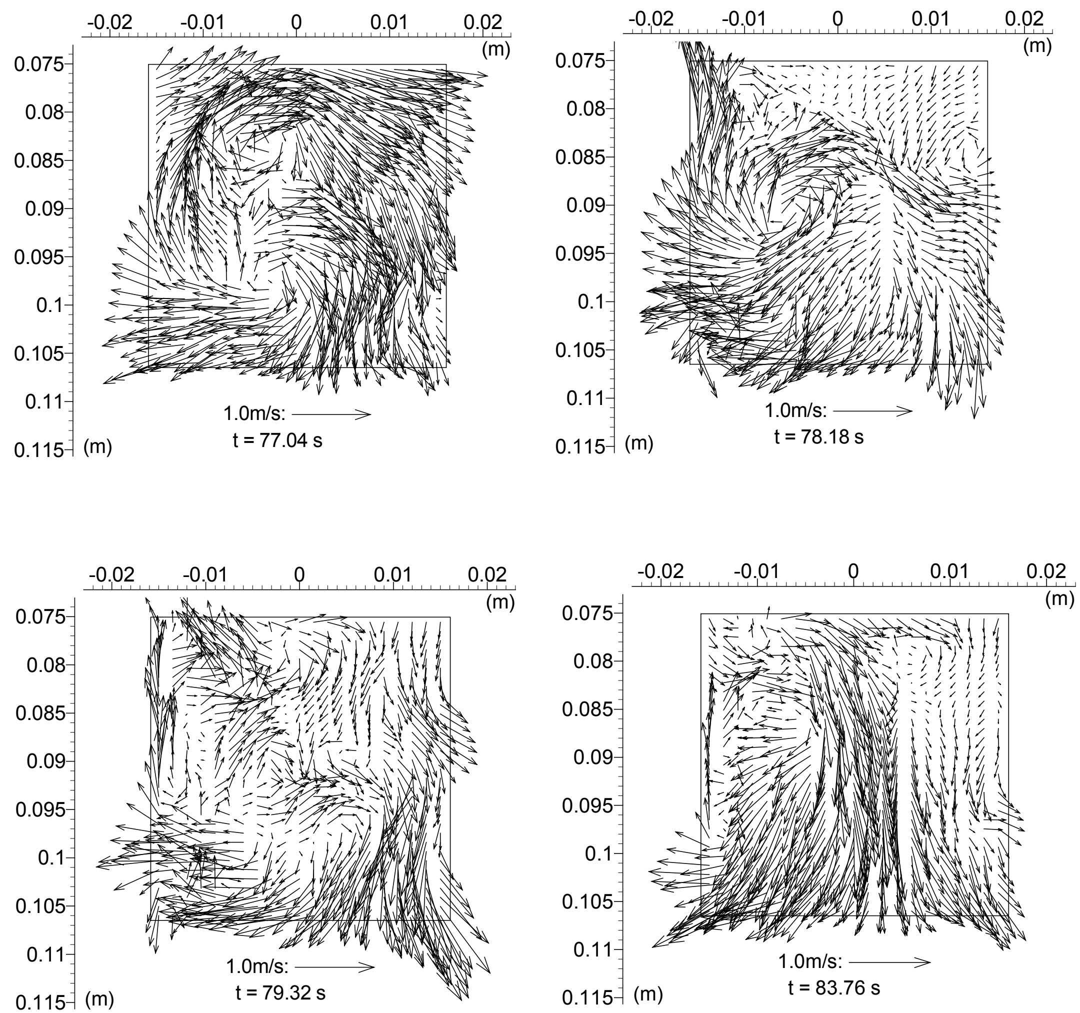

Evolution of flow pattern- view into nozzle port

Instantaneous Velocities in Mold Region

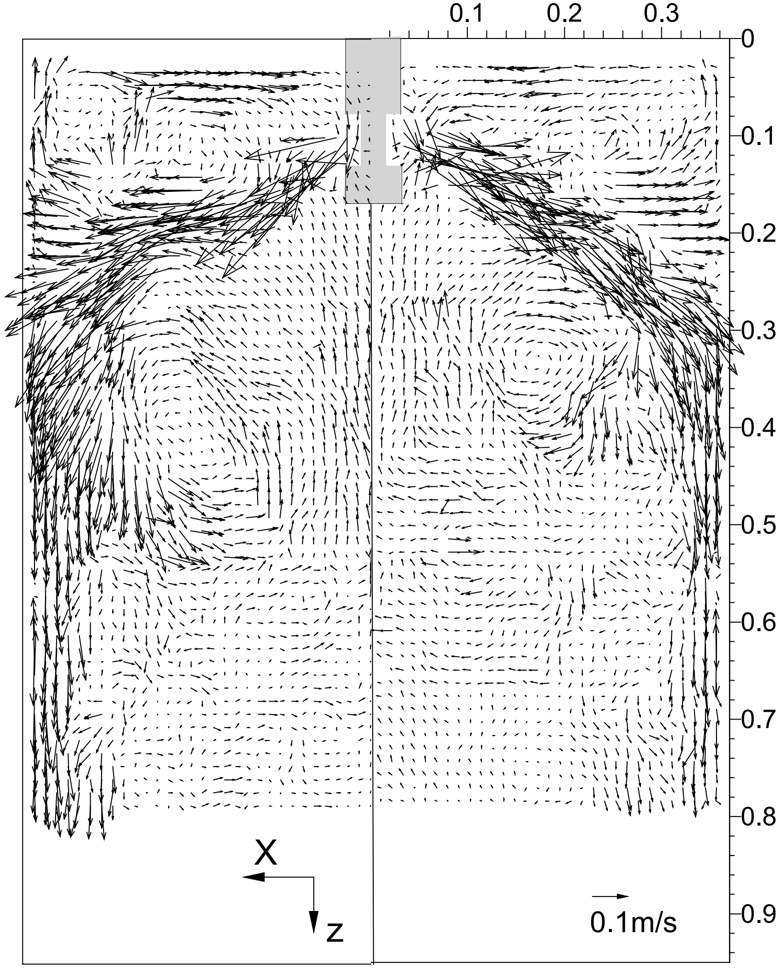

PIV (S. Sivaramakrishnan)

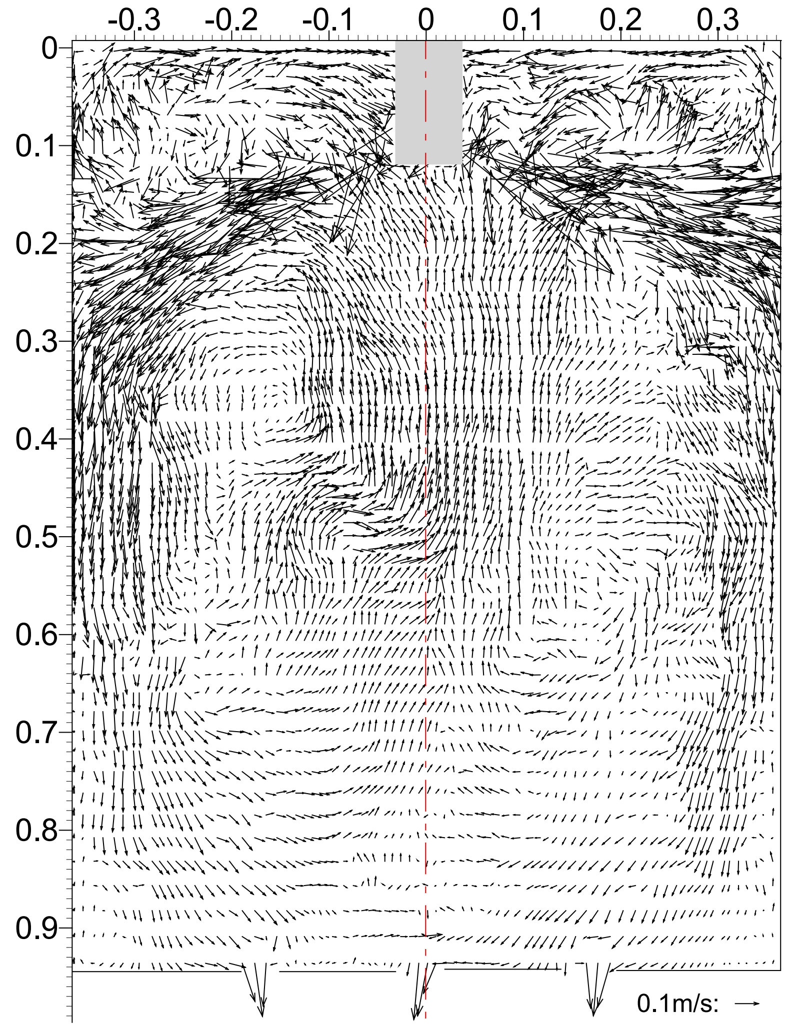

LES

Top Surface Velocity Fluctuation

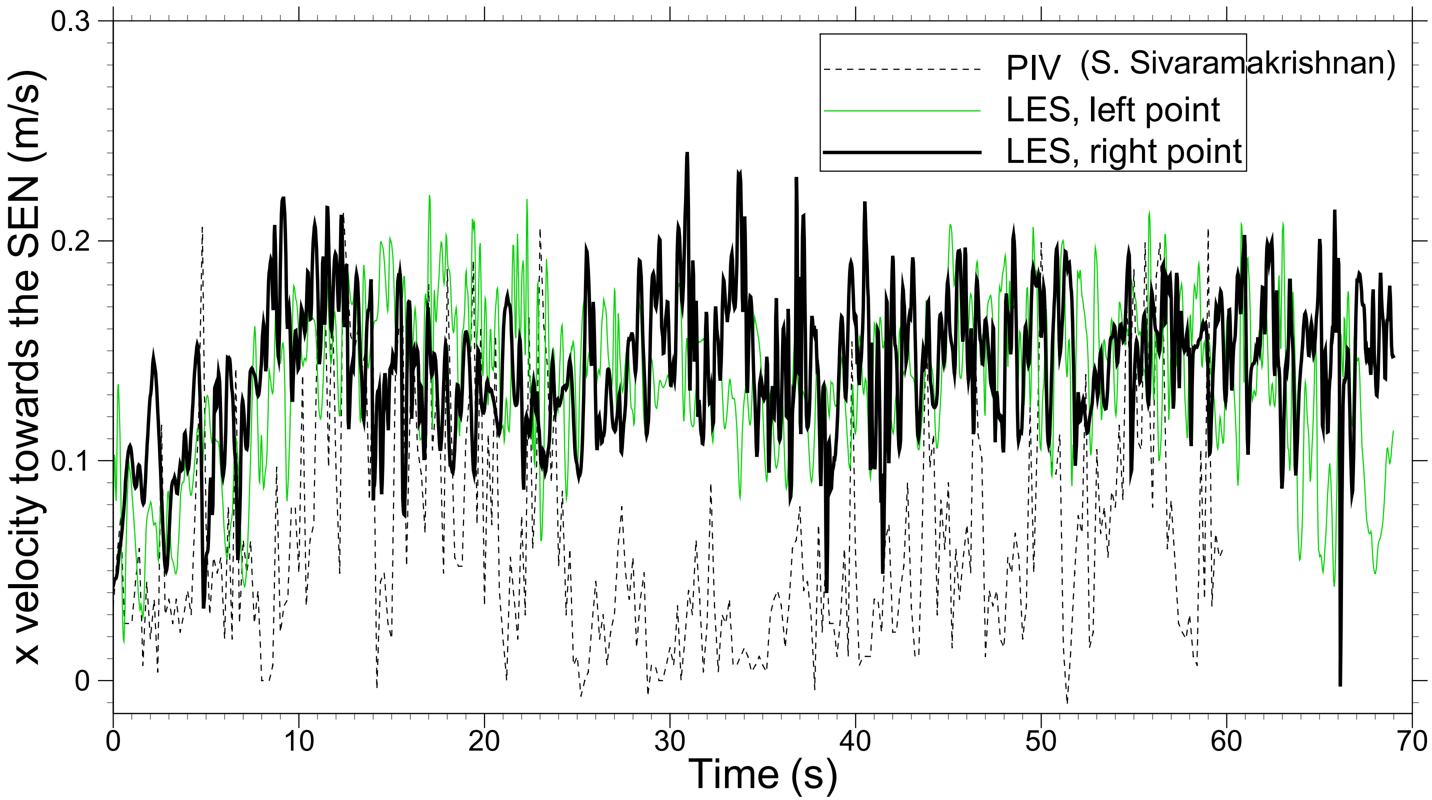

Horizontal velocity towards SEN at the point 20mm below top surface

mid-way between center and narrow face

Instantaneous Flow in Upper Roll Zone

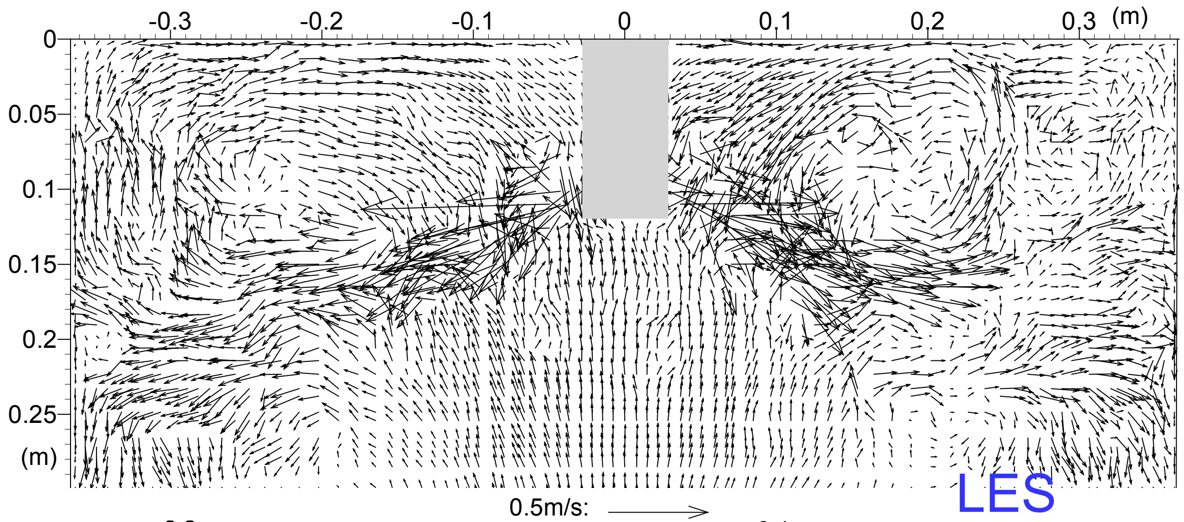

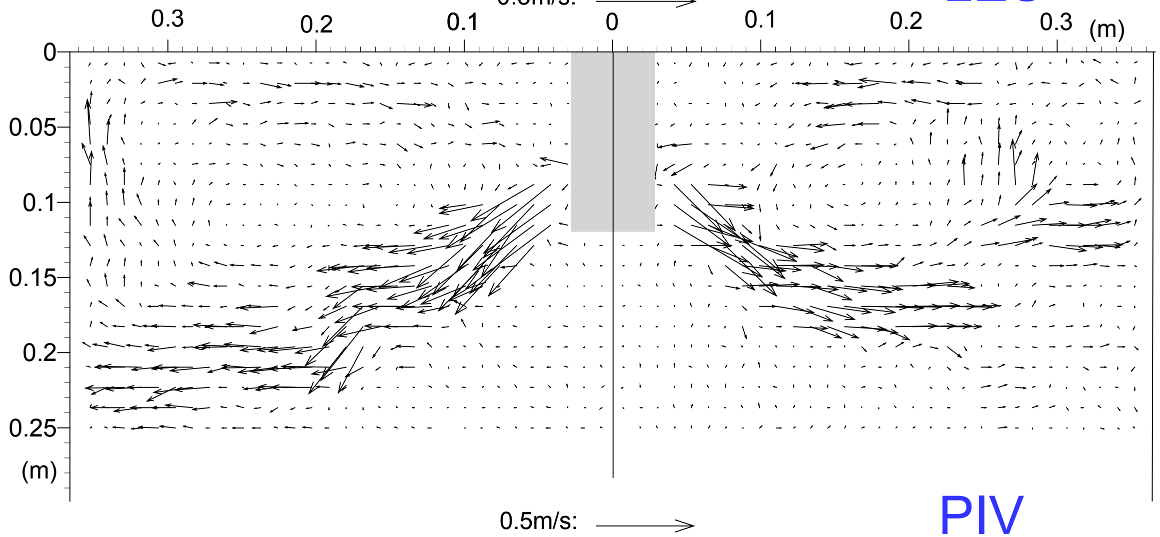

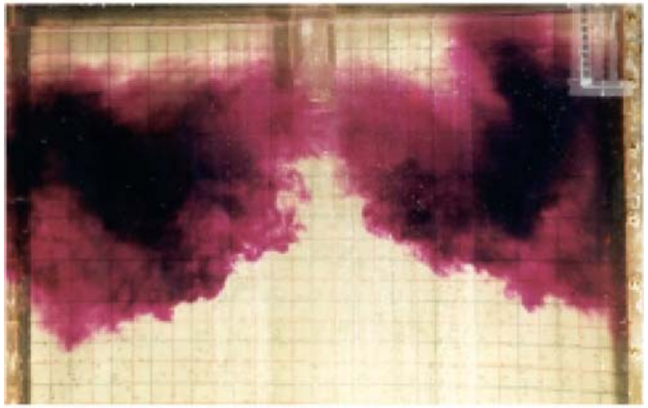

Dye injection

Time-Dependent Flow Structures in Lower Roll Region

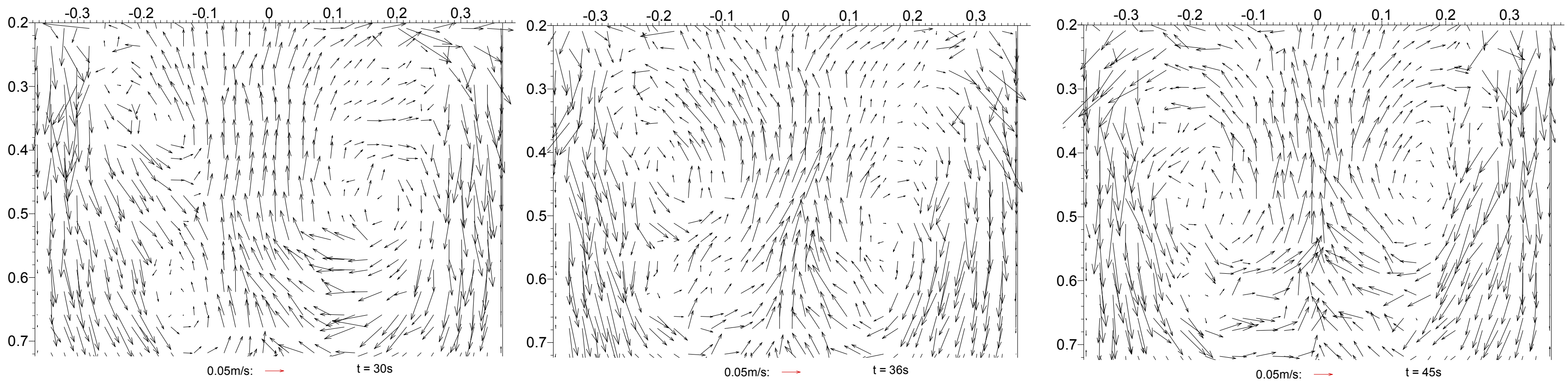

LES

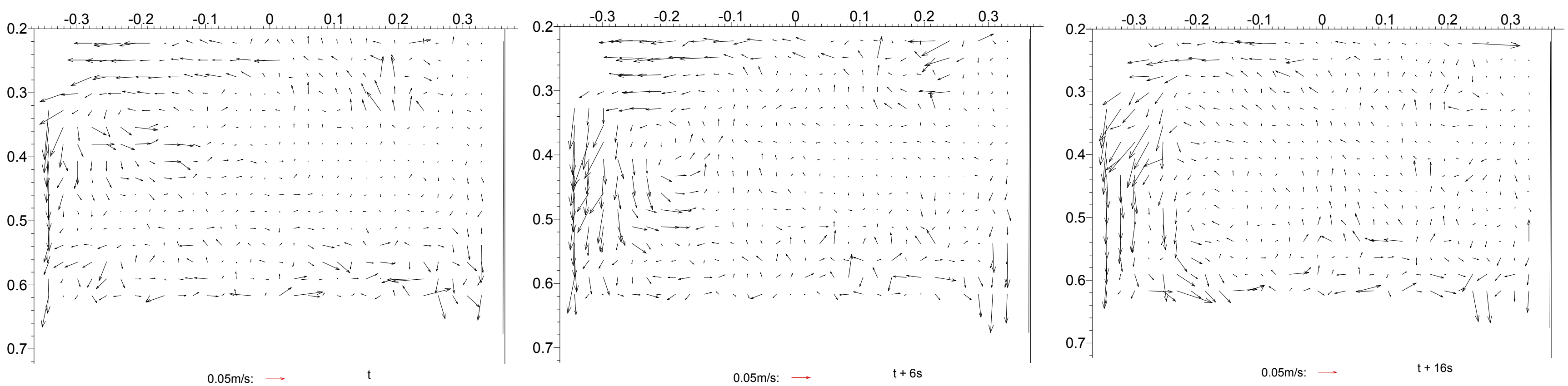

PIV

Simplified Simulations 1&2 (Half-Mold)

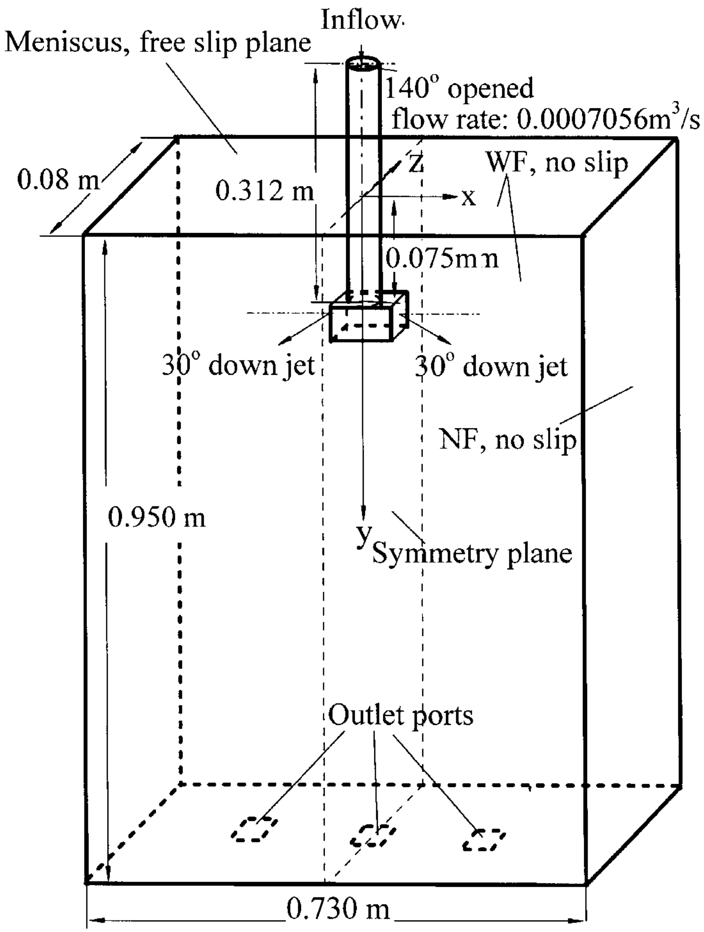

Schematics of simulation domain

Inflow velocities in cross-stream plane at nozzle port

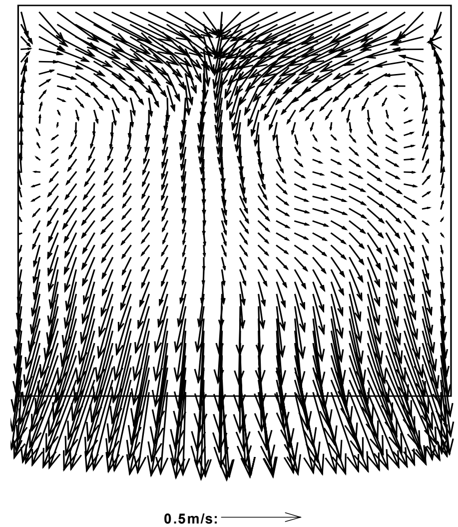

Simulation 1

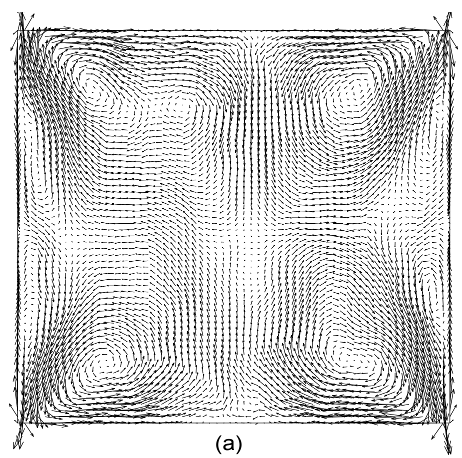

Simulation 2

Comparison of Time-Averaged Flow Fields in Mold Region

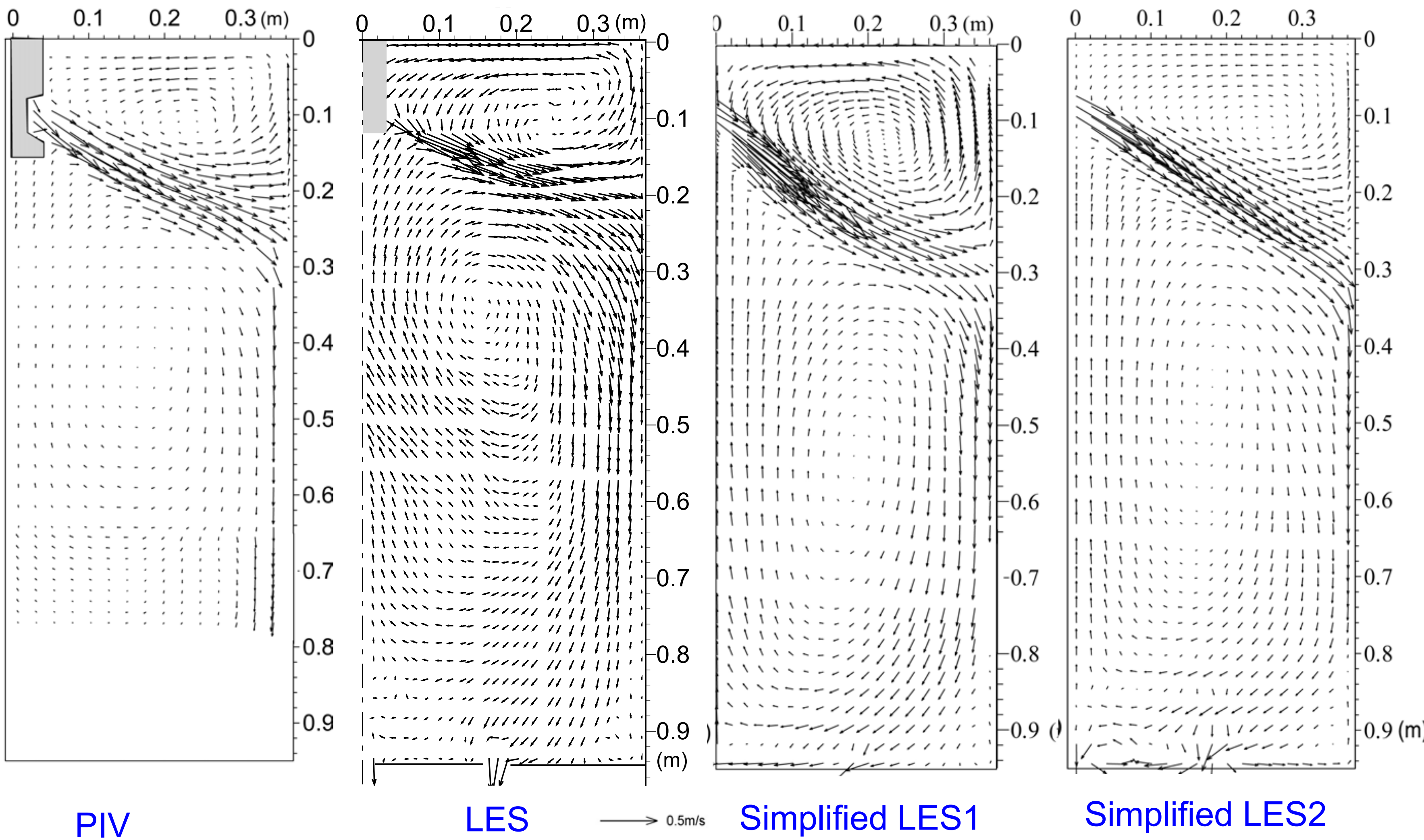

Velocities at center plane y = 0

Asymmetry in Lower Roll Region

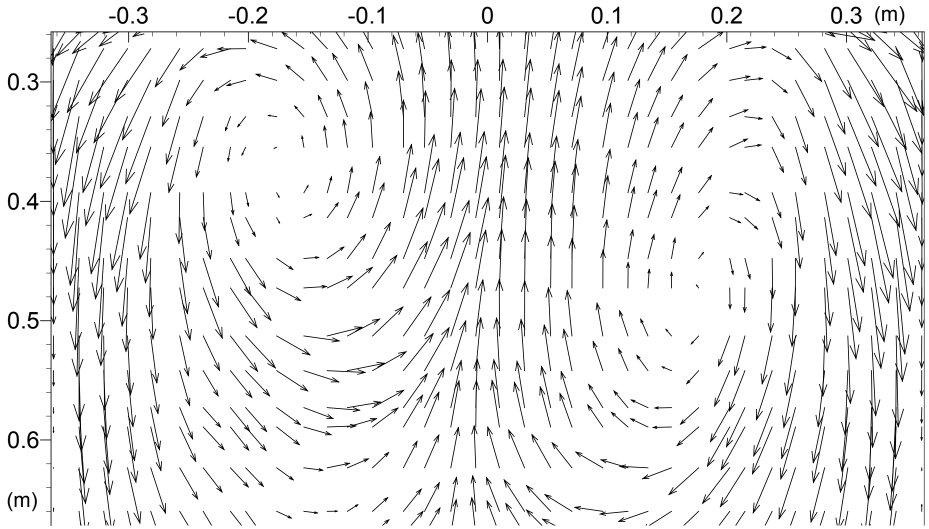

LES

Time-averaged velocity vectors in lower roll region at center plane y=0

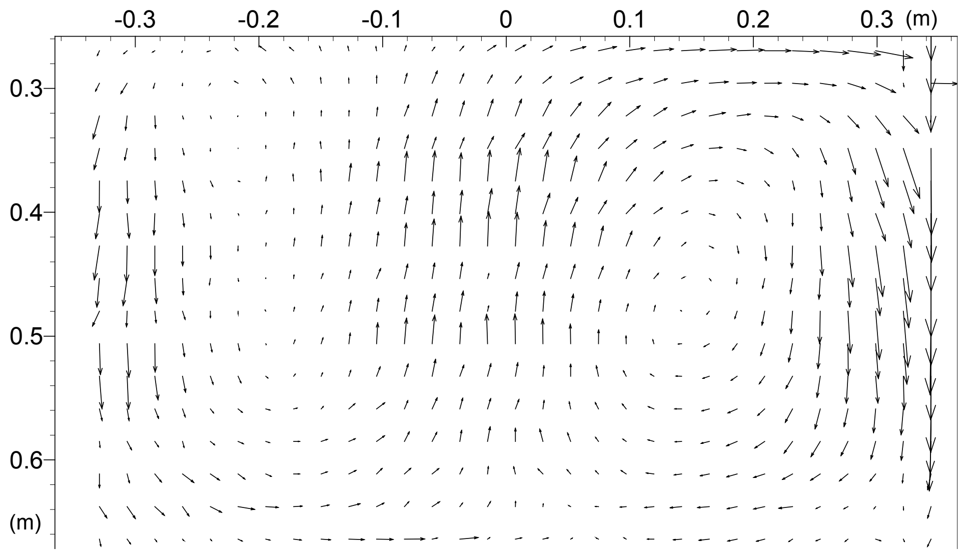

PIV

Half-Mold vs. Full-Mold Simlations

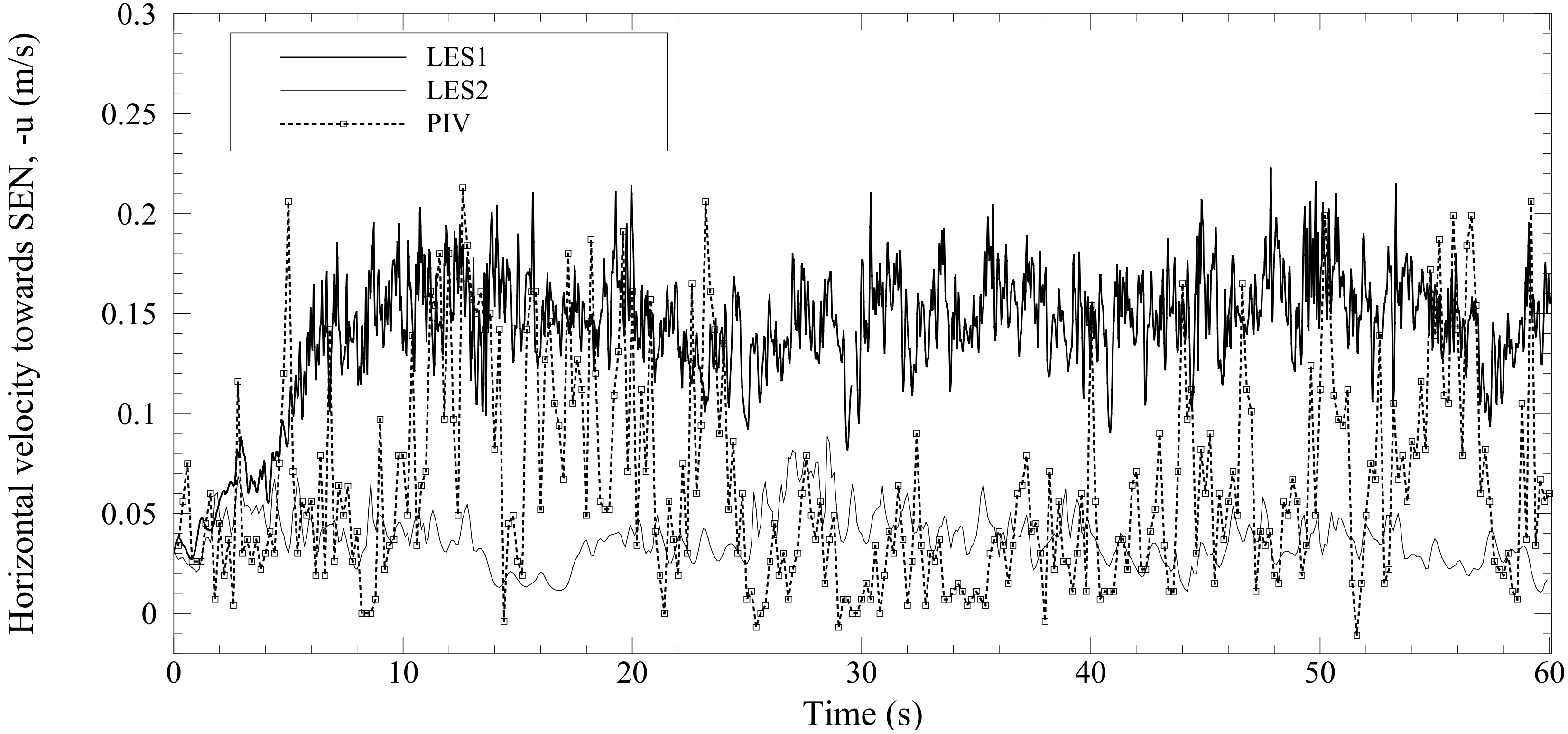

Two sides interaction is the main reason causing large fluctuation of top surface velocities.

Time-Averaged Velocities along Top Surface Centerline

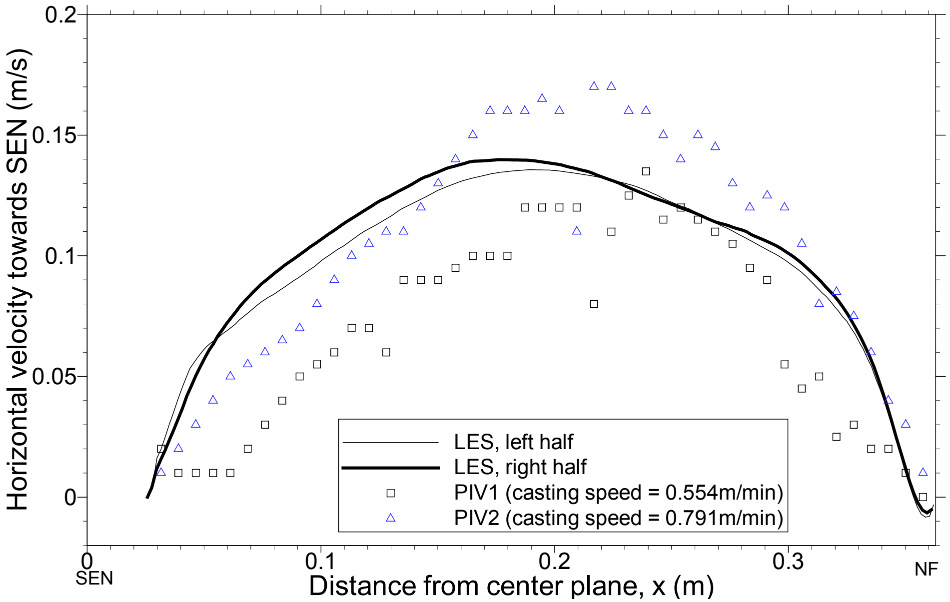

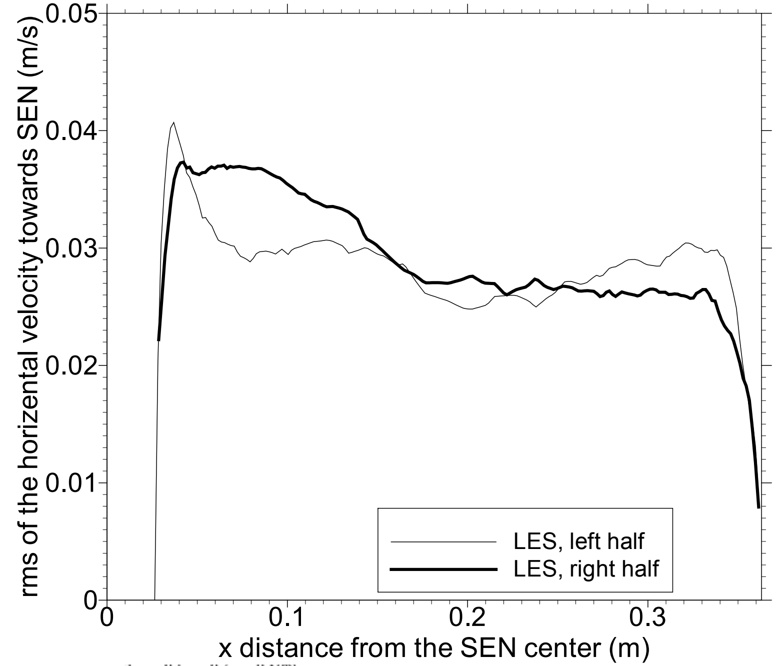

Time-averaged (left) and rms (right) velocities along centerline 3mm below top surface

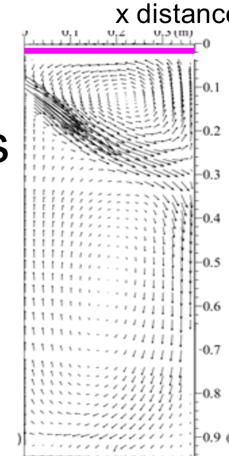

$$rms = \left(\frac{1}{(t_2 - t_1)} \sum_{t_i = t_1}^{t_2} \left(\mathrm{v}(\mathrm{t_i}) - \overline{\mathrm{v}} \right)^2 \Delta t \right)^{1/2}$$

PIV : S. Sivaramakrishnan, M.S. Thesis, 2000.

Velocity in Lower Roll Region

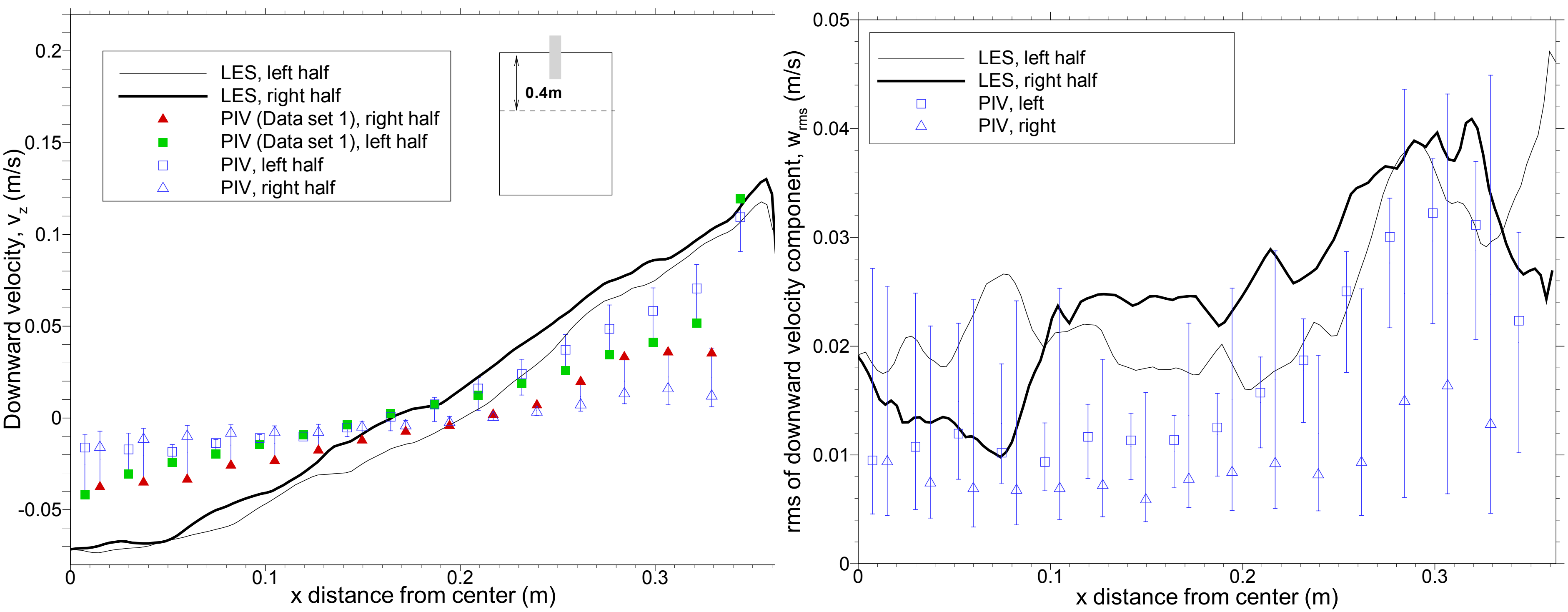

Time-averaged (left) and rms velocities along a horizontal line in lower roll region at center plane y=0

Observations

- LES predicted velocities agree well with PIV measurements
- The partial opening of the slide-gate induces a long, complex recirculation one in the SEN. Complex flow structures consisting of single and multiple vortices are seen to evolve in time at the outlet plane of the nozzle port.
- “Stair-step” and upward-bending flow patterns were observed in instantaneous jets.
- Significant asymmetry is seen in the instantaneous flow in the two halves of the mold cavity. Asymmetric flow structures are seen to persist longer than 200 seconds in the lower rolls in PIV.
- Level fluctuations near the narrow face occur over a wide range of frequencies, with the strongest having periods of ~7 and 11-25s. The instantaneous top surface velocity is found to fluctuate with sudden jumps from -0.01m/s to 0.24m/s occurring in as little as ~0.7s. These velocity jumps are seen in both the full nozzle-mold simulations and the PIV measurements.
- The velocity fields obtained from half-mold simulations with approximate inlet velocities generally agree with the results of the full domain simulations and PIV measurements. However, they do not capture the interaction between flows in the two halves, such as the instantaneous sudden jumps of top surface velocity.

Continuous Casting Consortium

Validation of Particle Transport Computation in a Full-Scale Water Model

Schematics of a Full-scale Water Model with Particle Removal Measurements

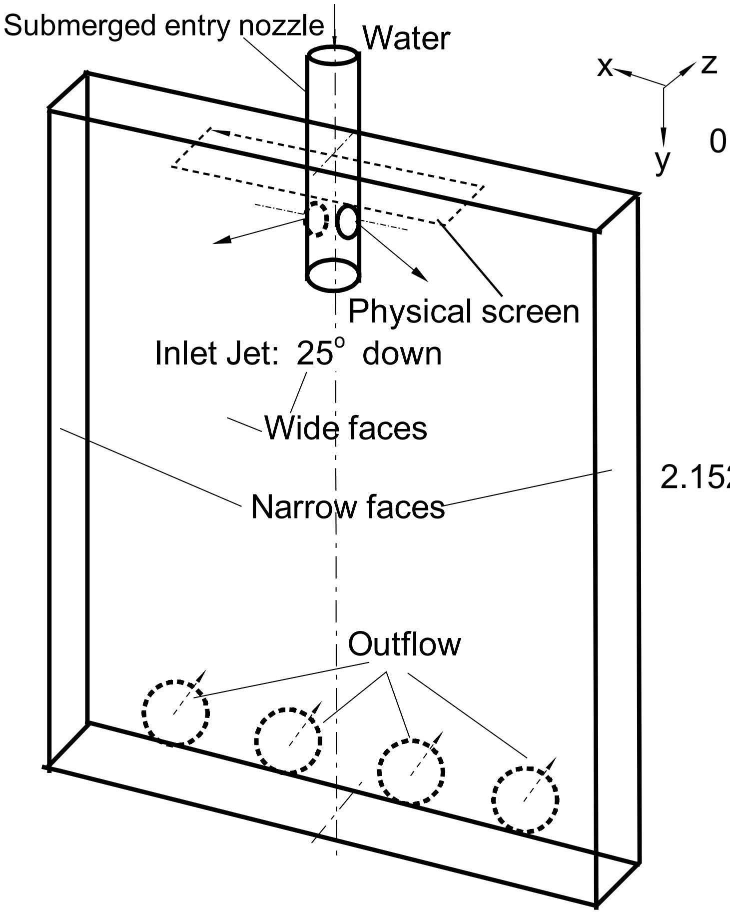

Physical water model

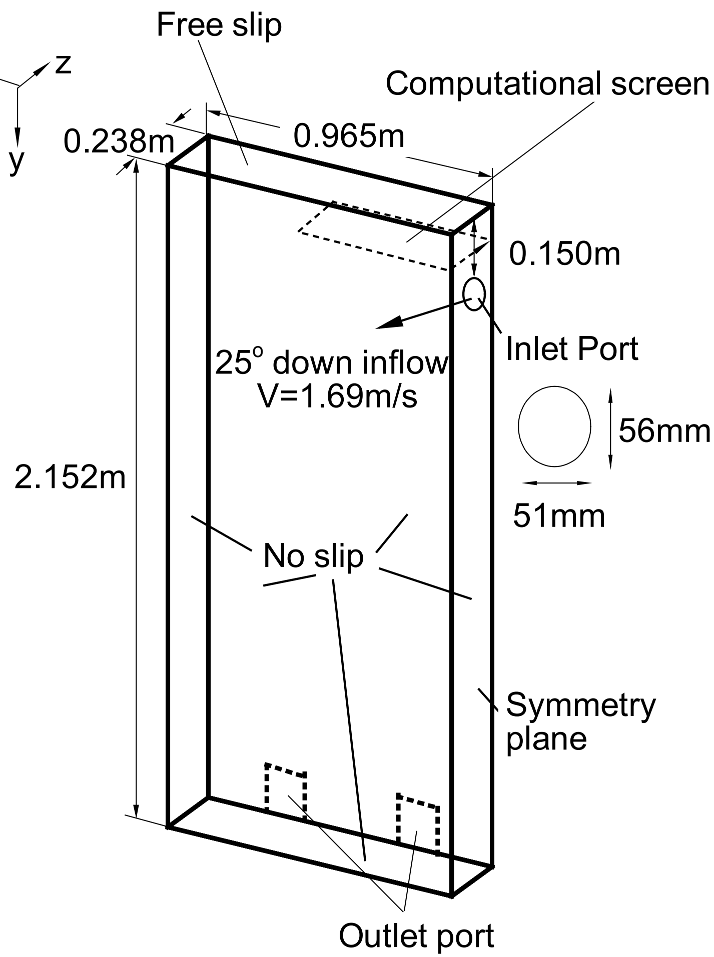

Computational domain

Simulation

Particle diameter: 3.8mm

Particle density: 988Kg/m^3

Particle injection:

Number of particles	Time
15,000	0-1.6s
500	2-2.4s
500	4-4.4s
500	6-6.4s
500	8-8.4s
500	10-10.4s

Inlet Velocities and Particle Initial Positions

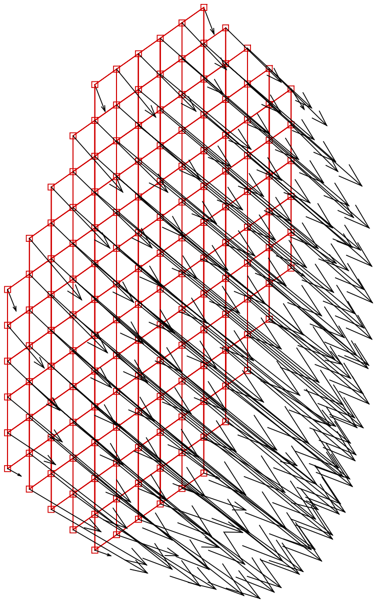

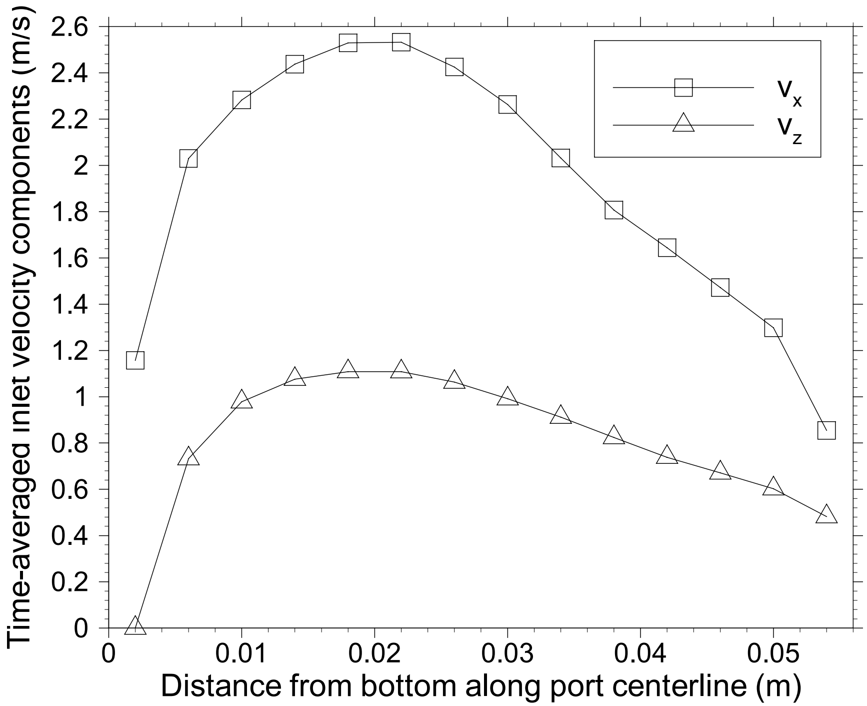

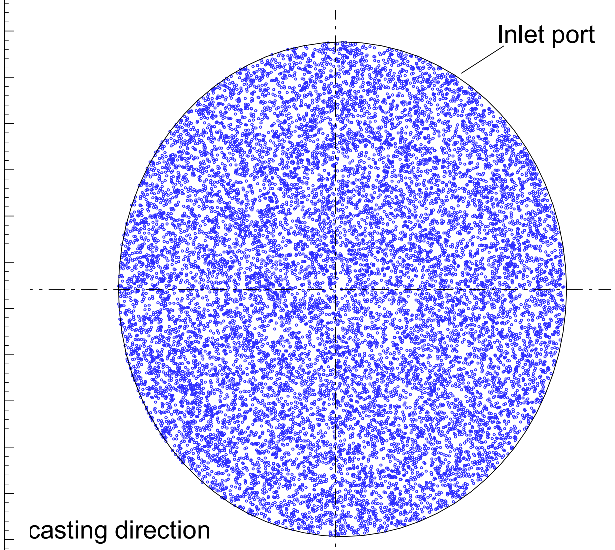

Time-averaged inlet velocities and initial distribution of particles at nozzle port in simulation.

Simulated Flow in Mold Region

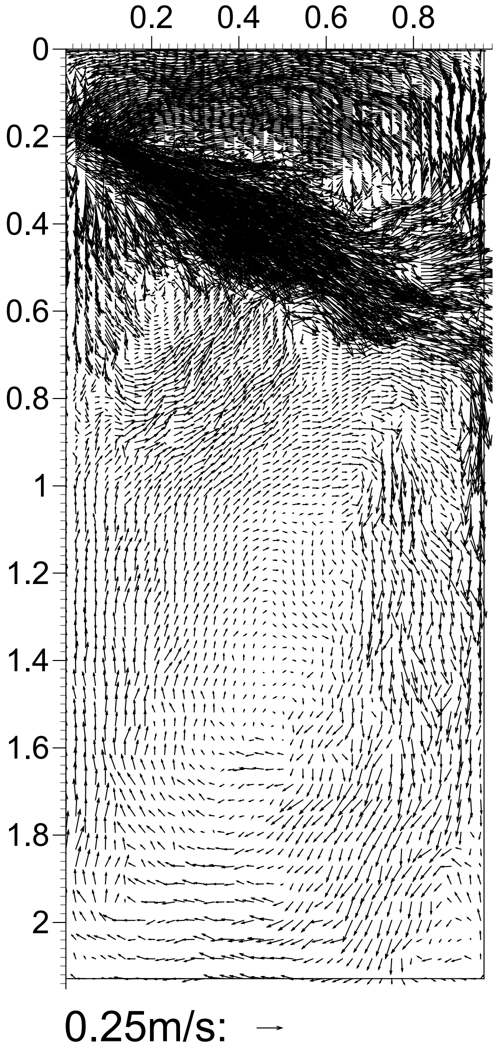

Instantaneous velocity field at y=0

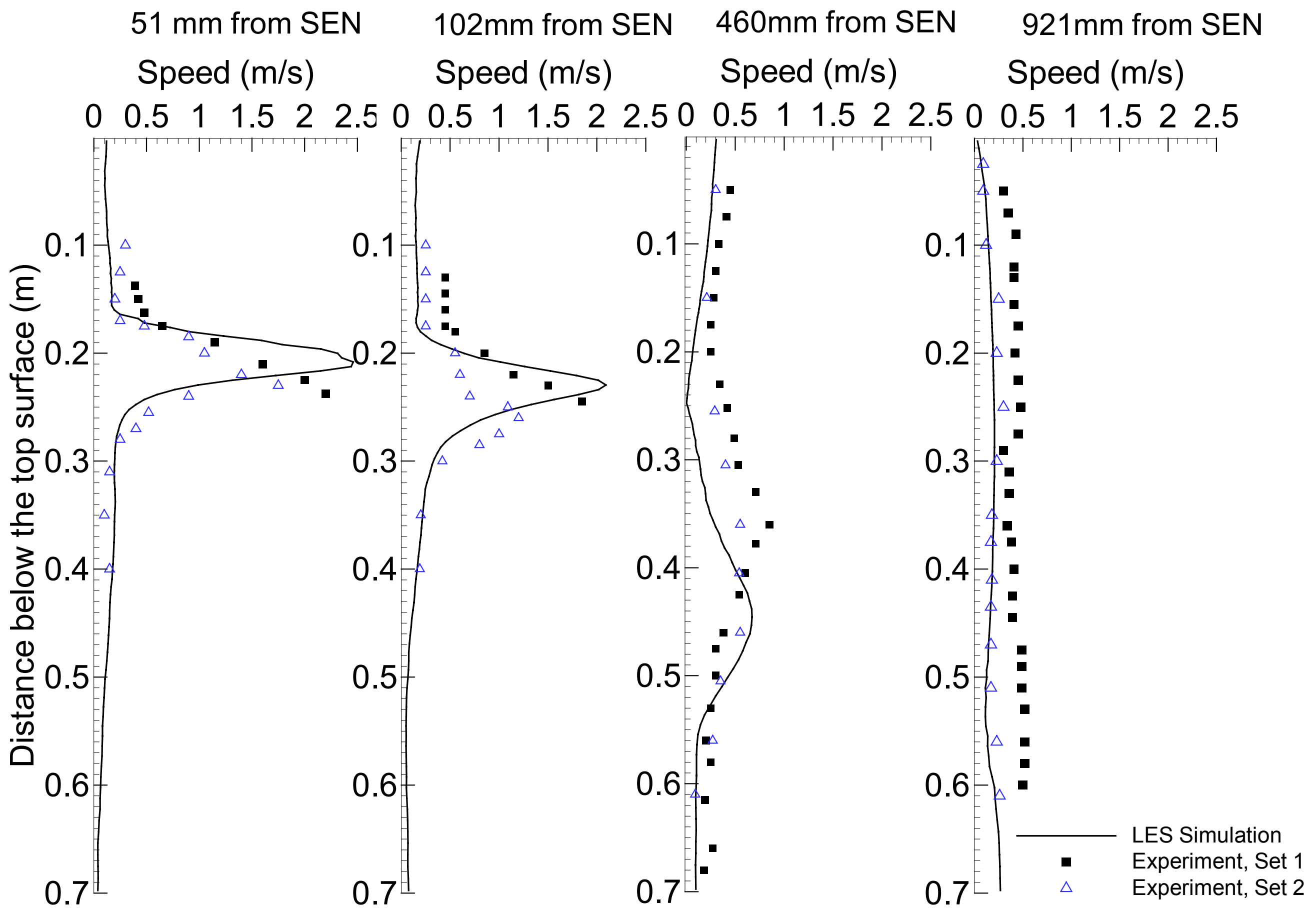

Comparison of time-averaged velocities along four vertical lines between LES and measurements.

Motion of All 15,000 Particles

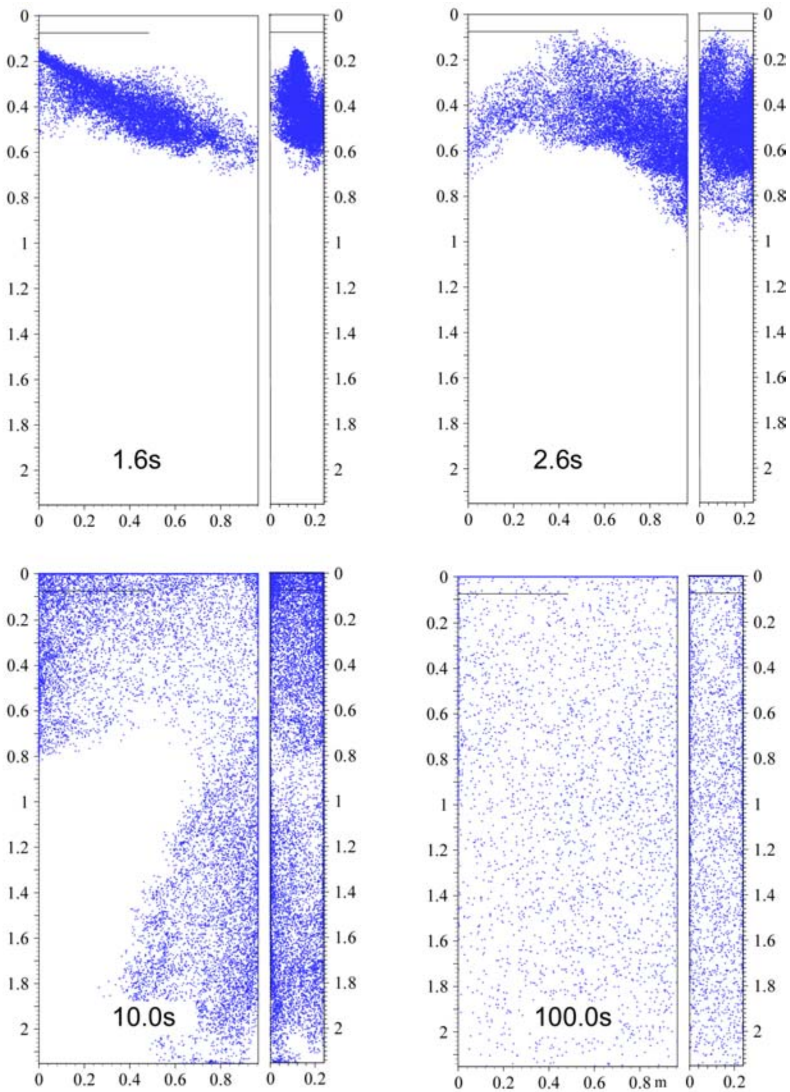

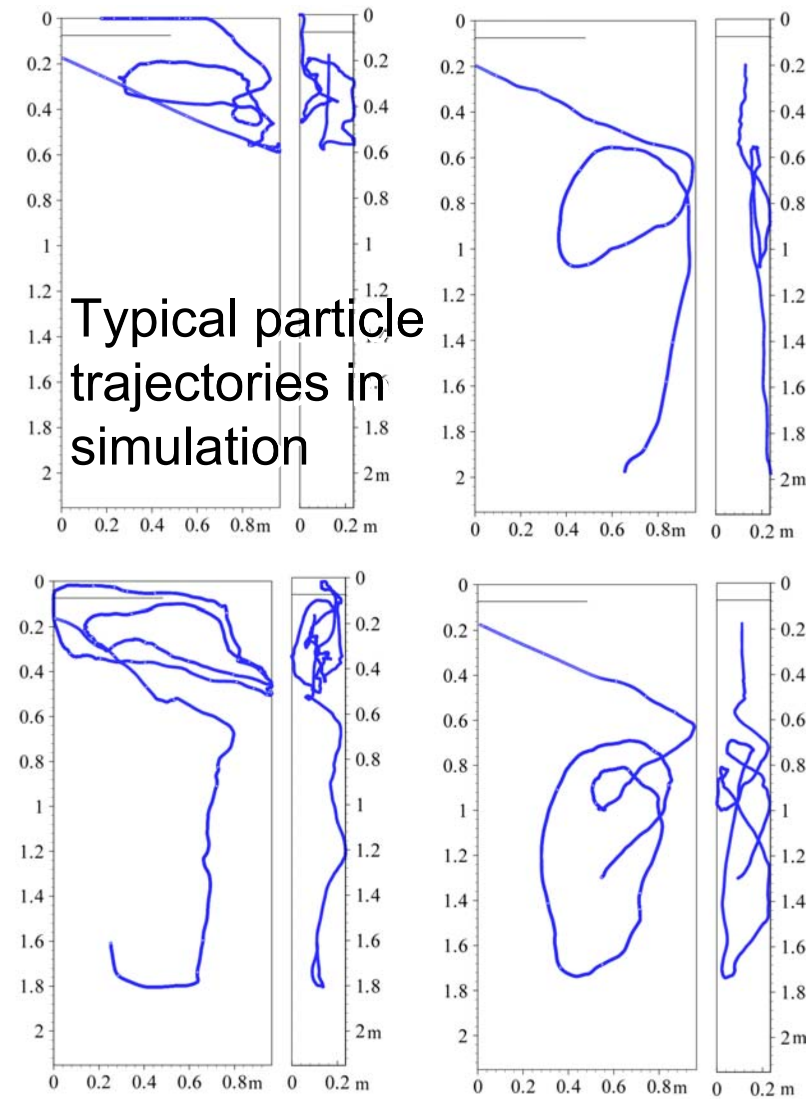

Typical particle trajectories in simulation

Particle Removal History

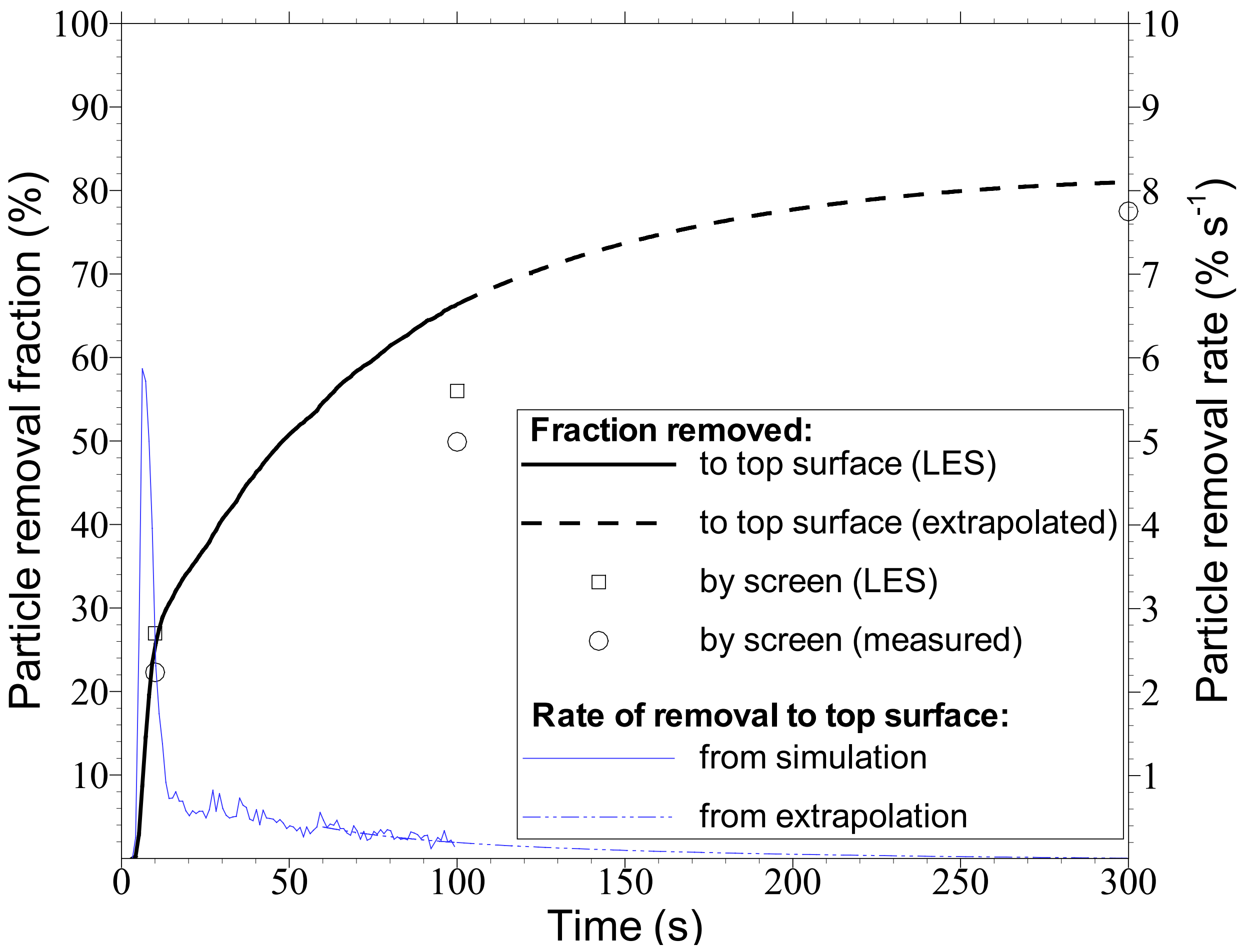

Simulation agrees with measurements.

Particle Removal Results (by Screen)

		0-10 seconds	10-100 seconds
LES	**500 particle groups**		
	1	27.2%	23.4%
	2	17.8%	27.2%
	3	26.2%	23.0%
	4	23.8%	23.2%
	5	33.0%	18.2%
	Average	**25.6%**	**23.0%**
	Standard Deviation	5.5%	2.9%
	2500 particle groups		
	1	27.2%	25.9%
	2	26.8%	27.1%
	3	20.0%	26.5%
	4	23.3%	27.8%
	5	31.8%	24.1%
	6	32.6%	24.9%
	Average	**27.0%**	**26.1%**
	Standard Deviation	4.8%	1.4%
Experiment		**22.3%**	**27.6%**

Observations:

A comparison of particle removal fractions obtained from 2,500 and 500 particle groups suggests that increasing the number of particles improves the accuracy of removal predictions for later times (e.g. 10-100s). At least 2500 particles are required to obtain accuracy within ±3%. Particle removal at early times (e.g. ≤10s) is governed by chaotic fluctuations of the flow, which generate variations of ±5%.

Continuous Casting Consortium

Simulation of Time-Dependent Flow in an Actual Thin-Slab Steel Caster and Its Corresponding Water Model

Schematics of Computational Domains

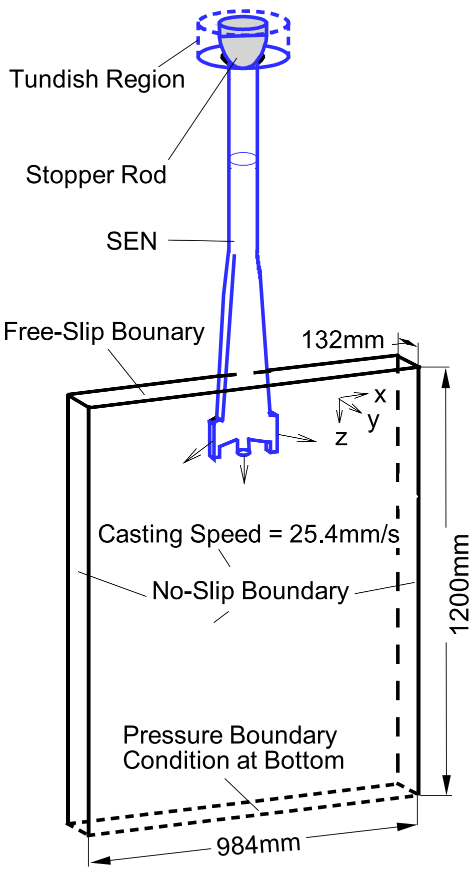

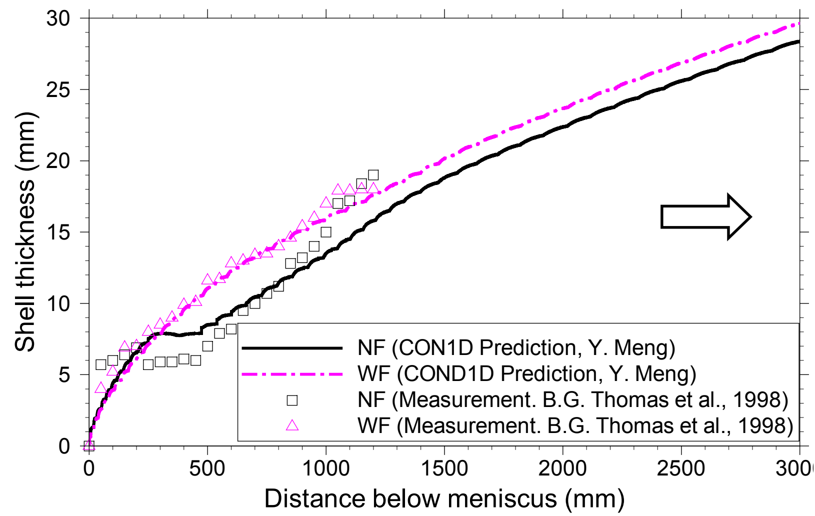

Shell thickness obtained from CON1D prediction (Y. Meng), compared with measurements (B.G. Thomas et al, 1998)

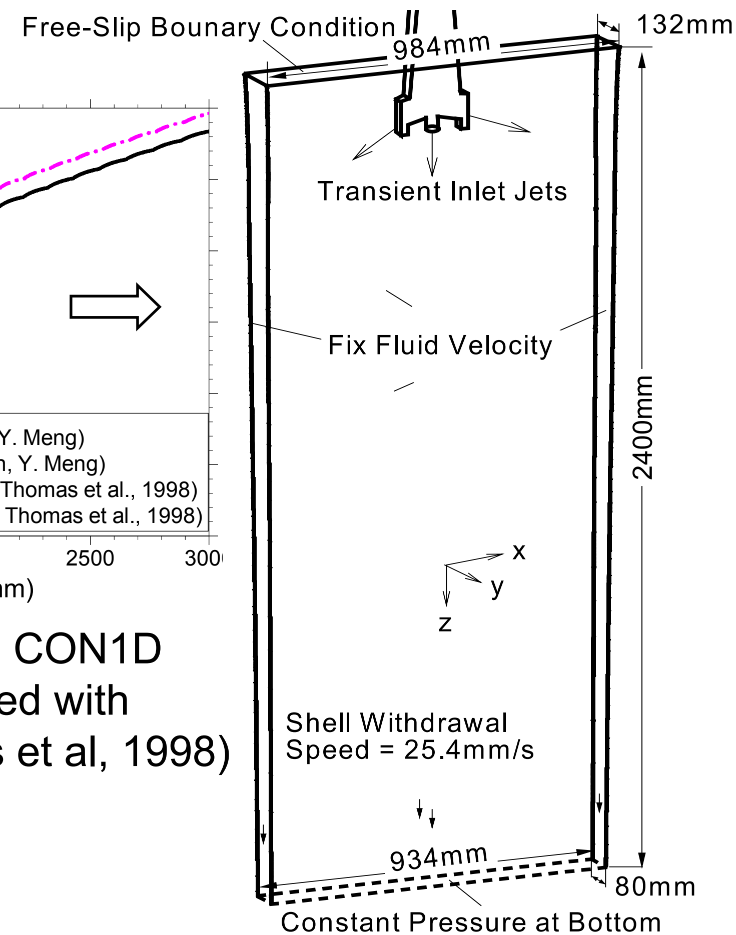

Computational domain of the corresponding water model

Computational domain of steel caster

Modeling Solidification Effects on Flow

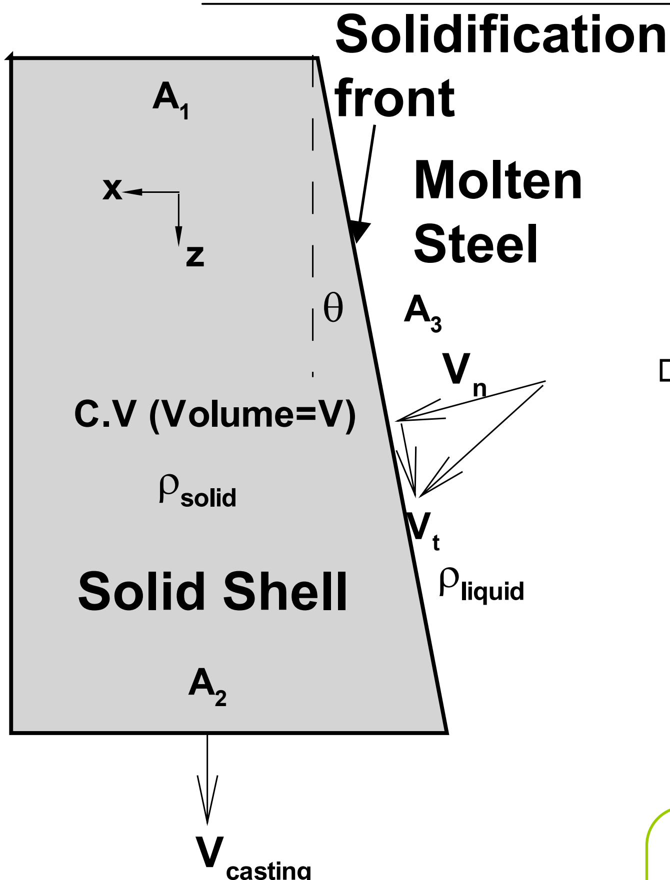

Eulerian Frame

Assumption:
Constant solid density
Constant shell thickness

Mass Conservation:

$$\frac{\partial(\rho_s \mathrm{V})}{\partial t}dt = \left(\rho_s A_1 V_{casting} + \rho_l A_3 V_n - \rho_s A_2 V_{casting}\right)dt$$

$$\Rightarrow V_n = \frac{\rho_s (A_2 - A_1)}{\rho_l A_3} V_{casting} = \left(\frac{\rho_s}{\rho_l}\sin\theta\right) V_{casting}$$

No-slip tangential to solidification front

$$V_t = V_{casting}\cos\theta$$

Velocity boundary condition at shell front location:

$$V_x = V_n\cos\theta - V_t\sin\theta = \left(\frac{\rho_s}{\rho_l} - 1\right)\sin\theta\cos\theta V_{casting}$$

$$V_z = V_n\sin\theta + V_t\cos\theta = \left(\frac{\rho_s}{\rho_l}\sin^2\theta + \cos^2\theta\right)V_{casting}$$

Transient Velocities near Stopper Rod

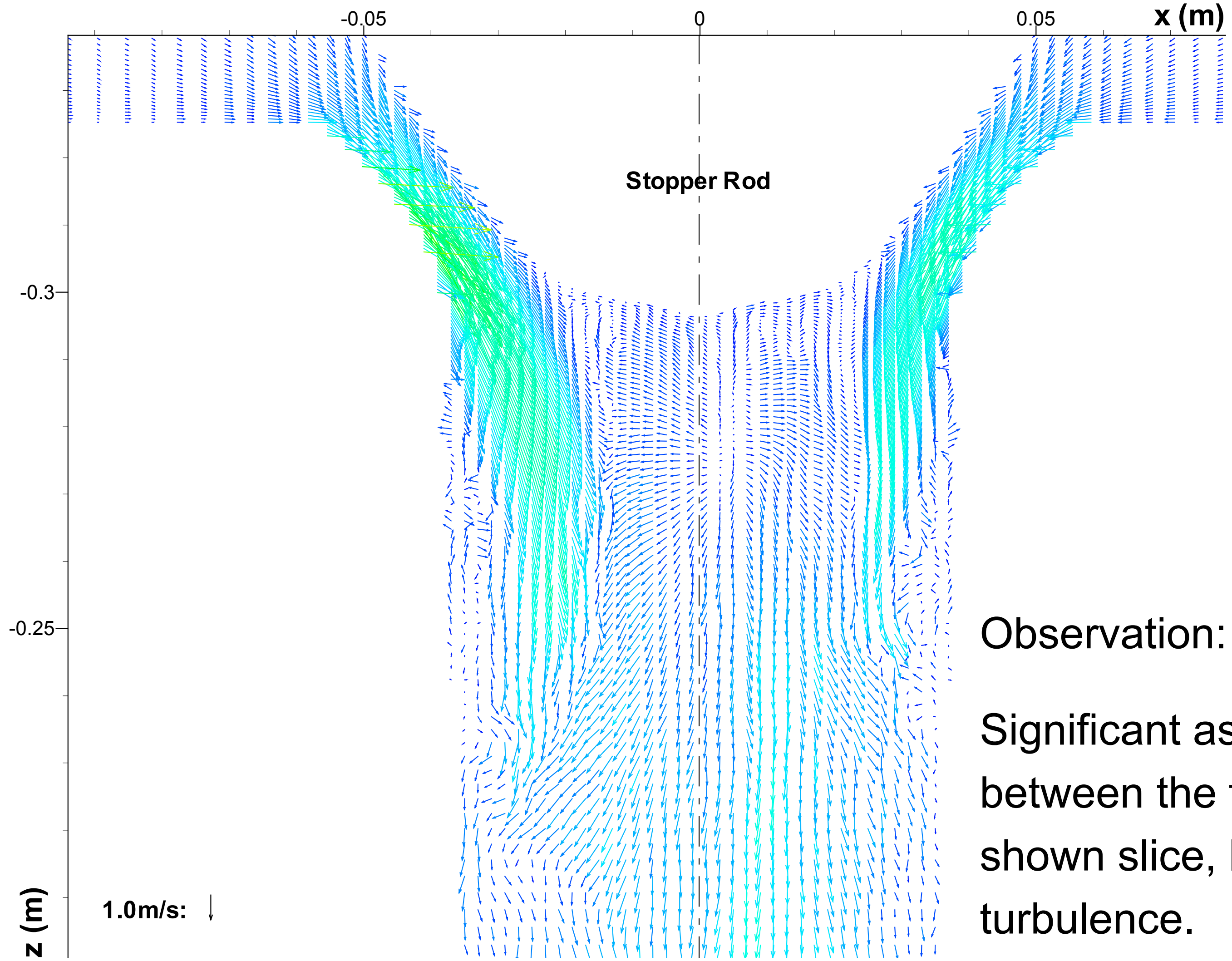

Observation:

Significant asymmetry observed between the flow on the two sides at shown slice, likely due to non-ergodic turbulence.

Instantaneous Flow near Nozzle Port

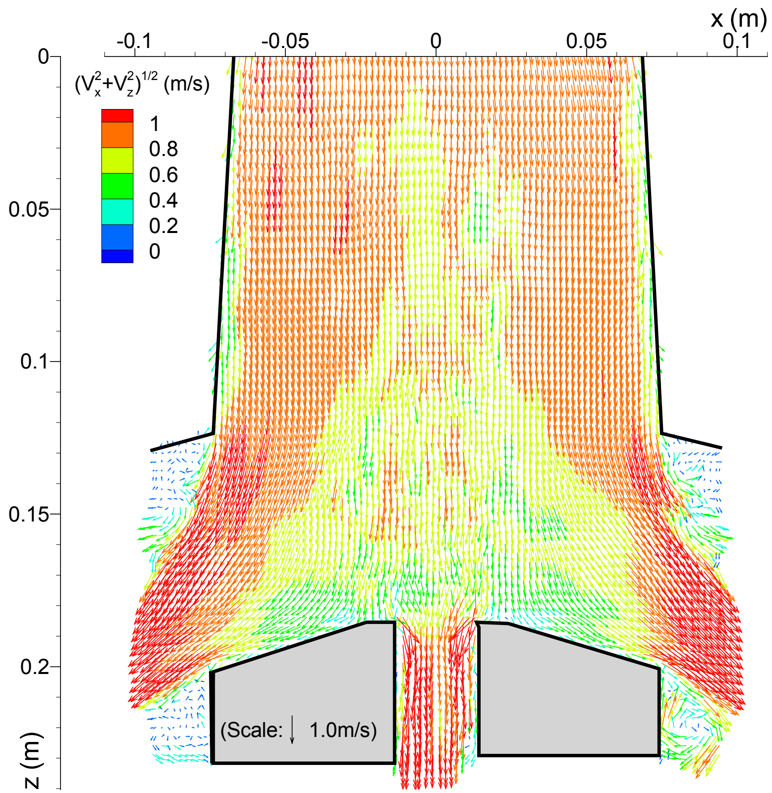

Deep jet angle on both sides

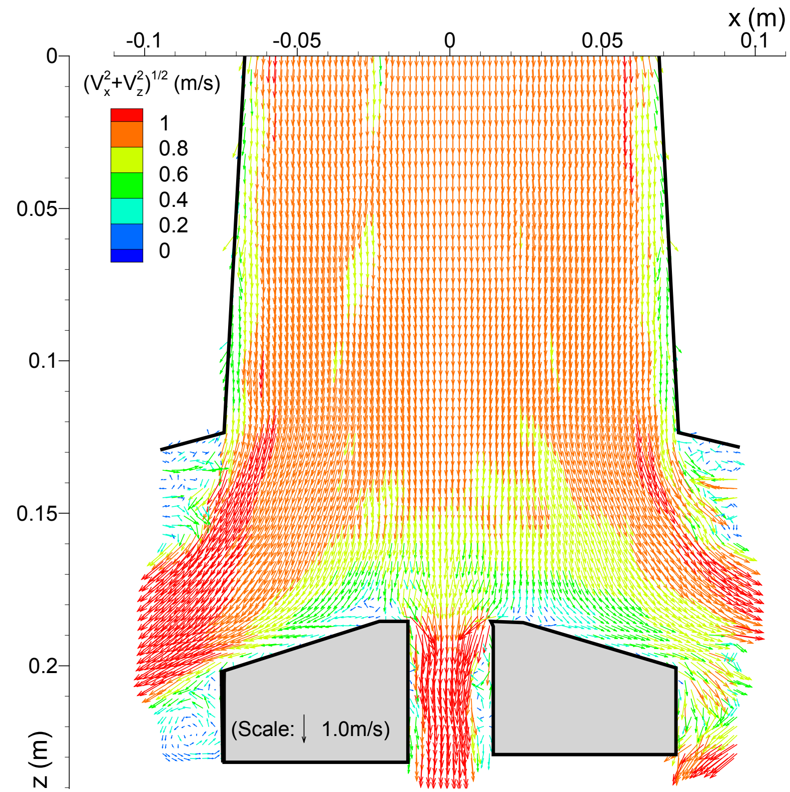

Asymmetrical jets

Time-Averaged Velocities Along Port Centerlines

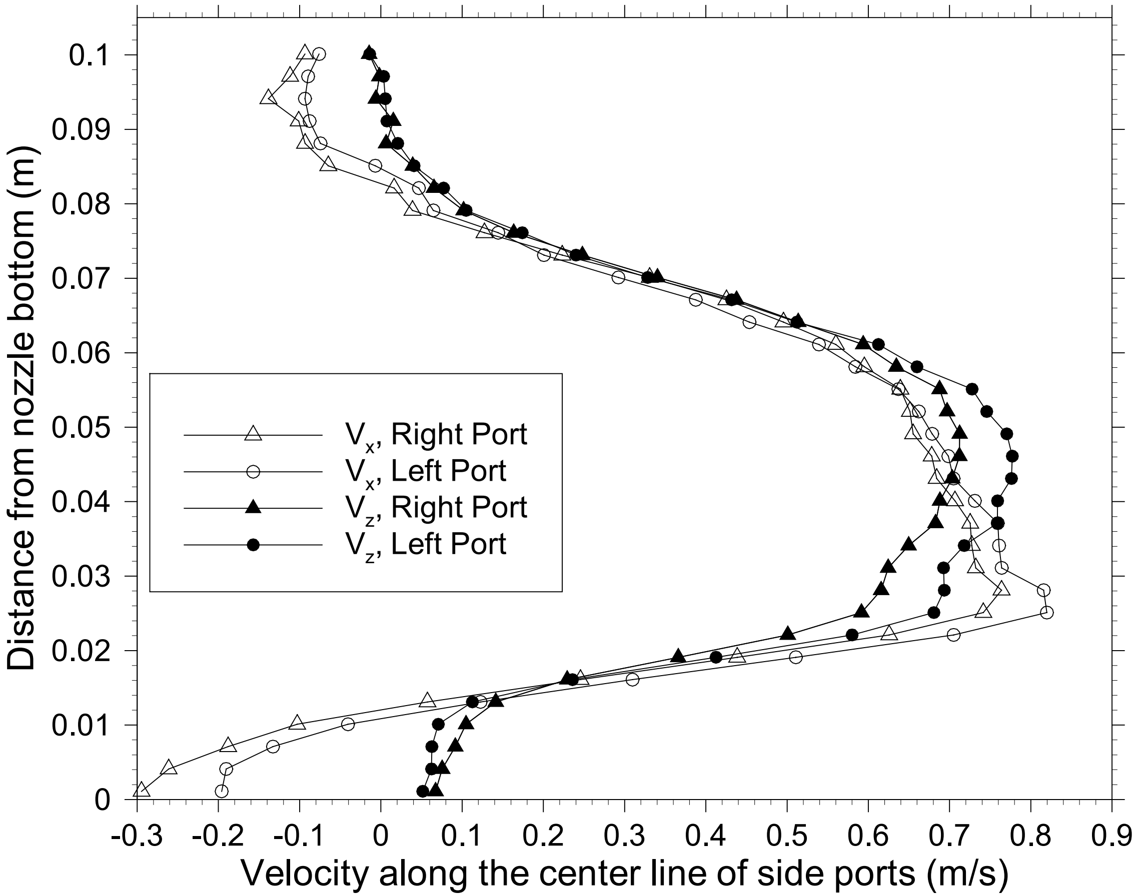

Transient Flow in Water Model

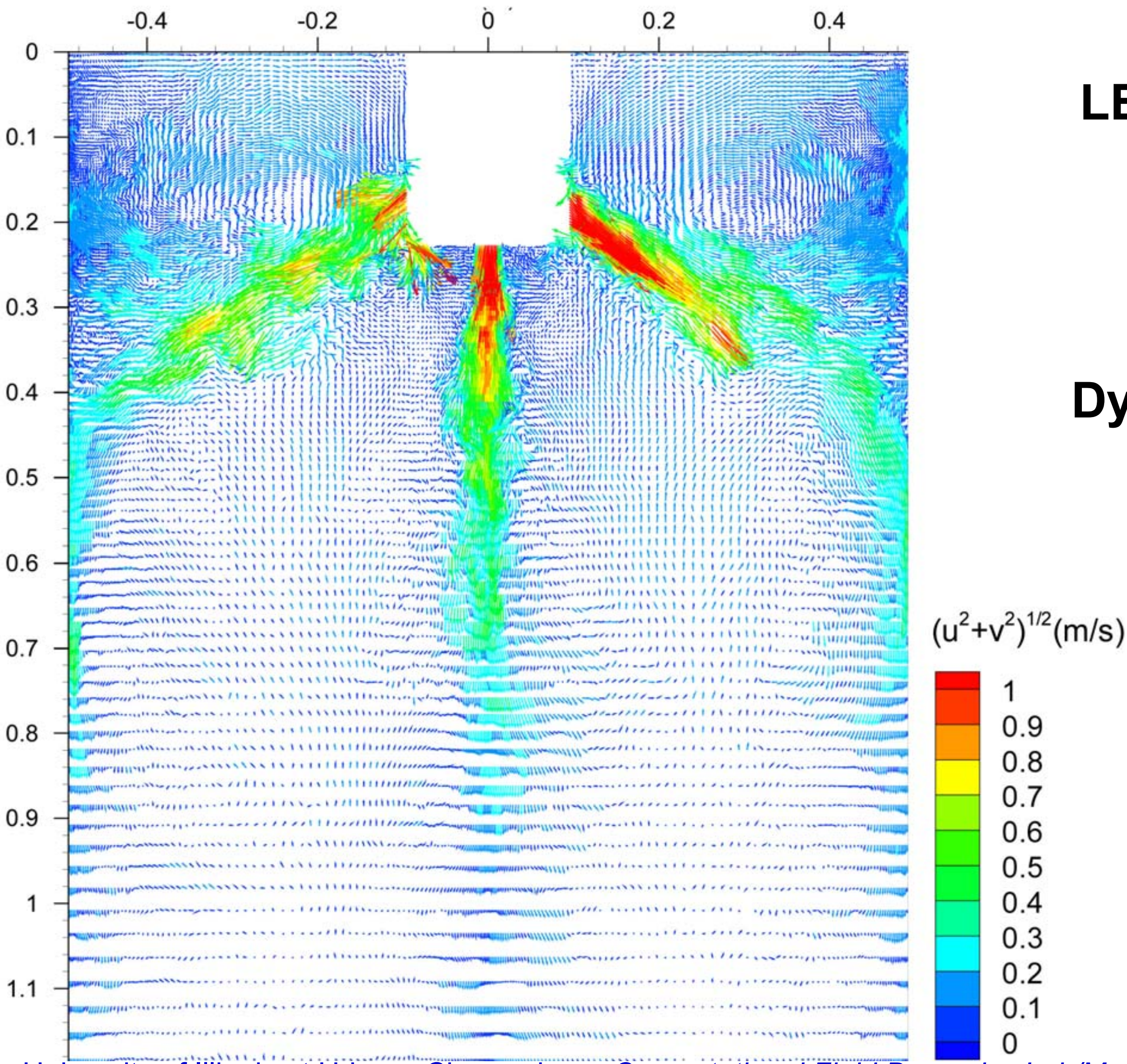

LES

Video Clip

Dye injection (Dr. R. O'Malley)

Time Averaged Fluid Velocity Field (~50s)

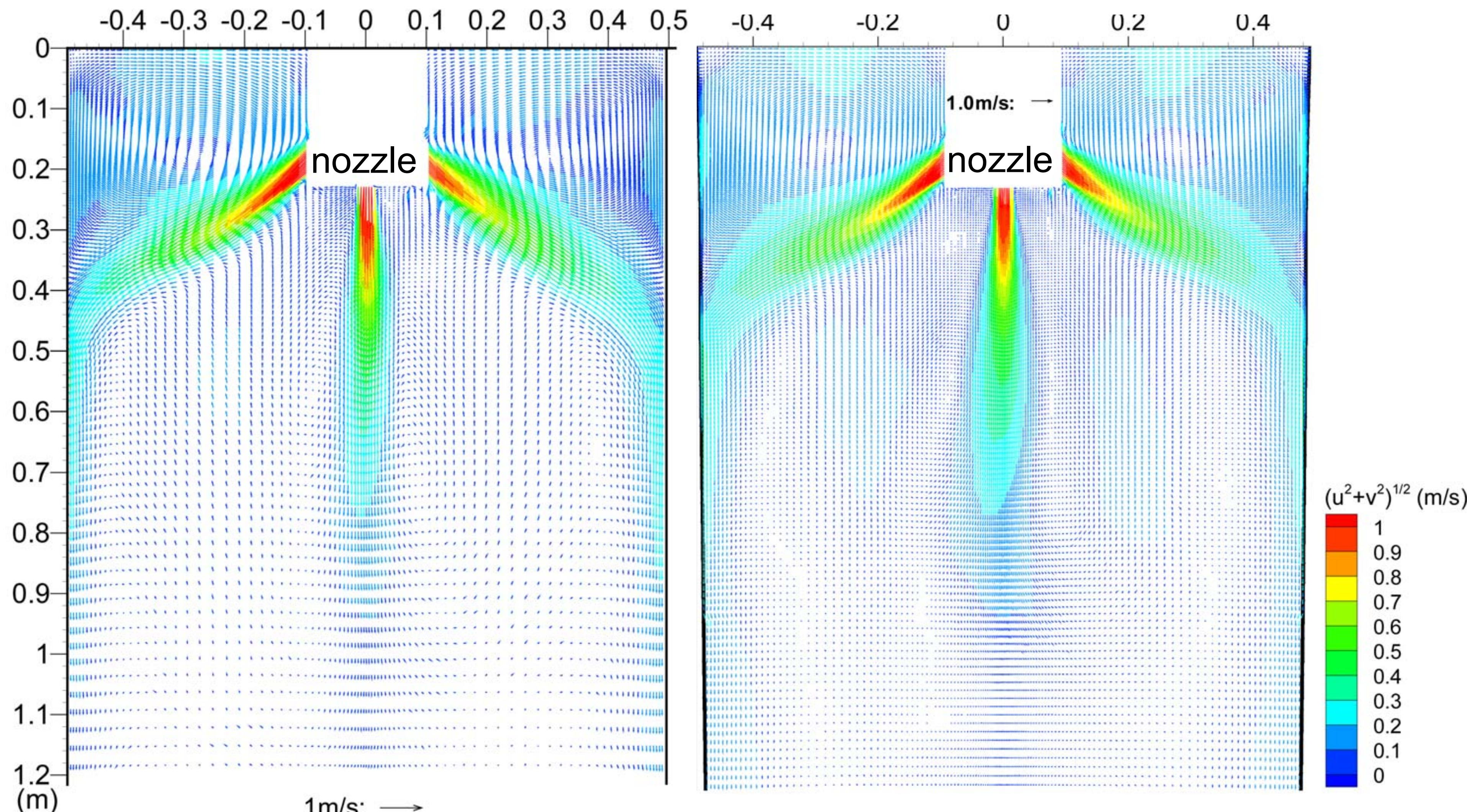

Water Model **Steel Caster**

Center Nozzle Port Effects on Flow in Mold Region

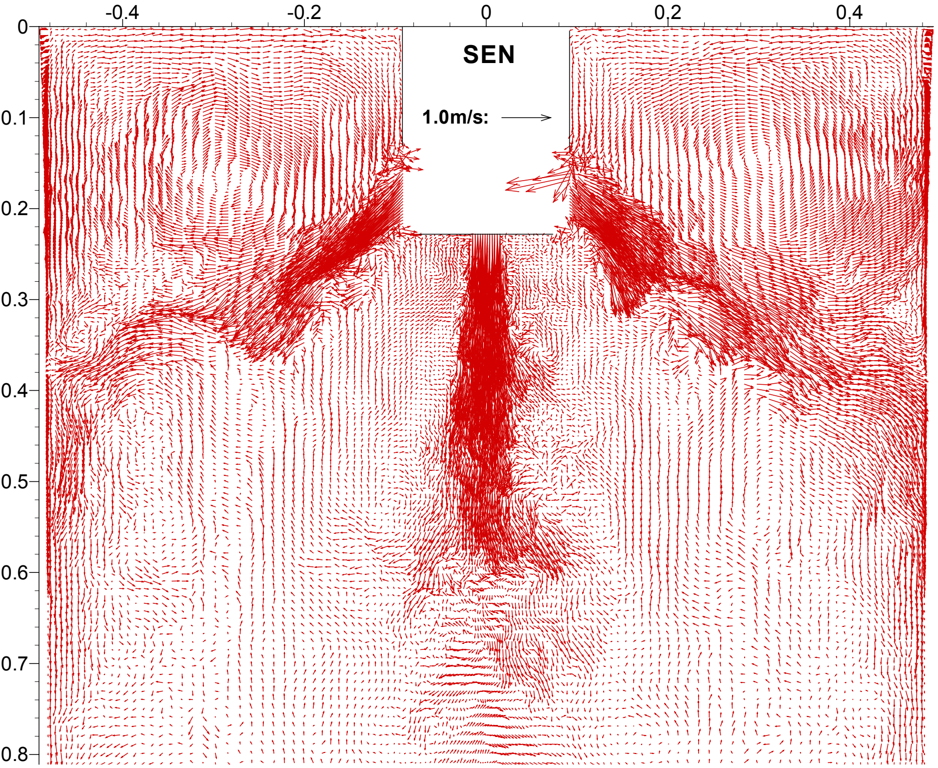

Flow with center nozzle port

(same time instant as right plot)

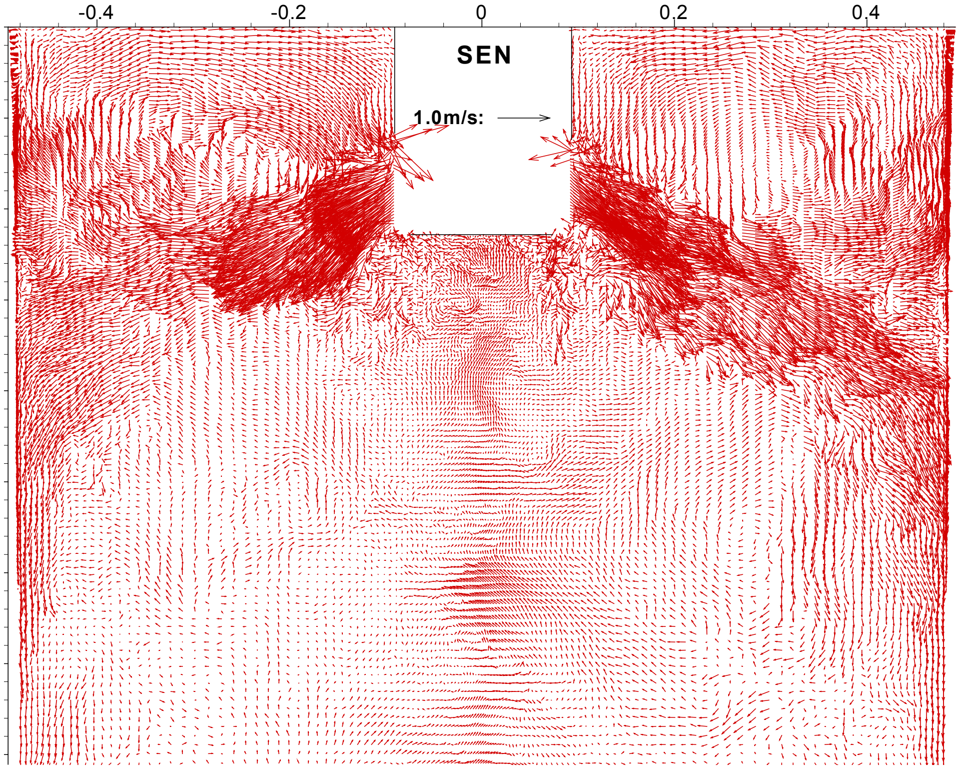

Flow with center nozzle port blocked

(3.4 s after blocking)

Center Nozzle Port Effects on Flow in Mold Region (ctd.)

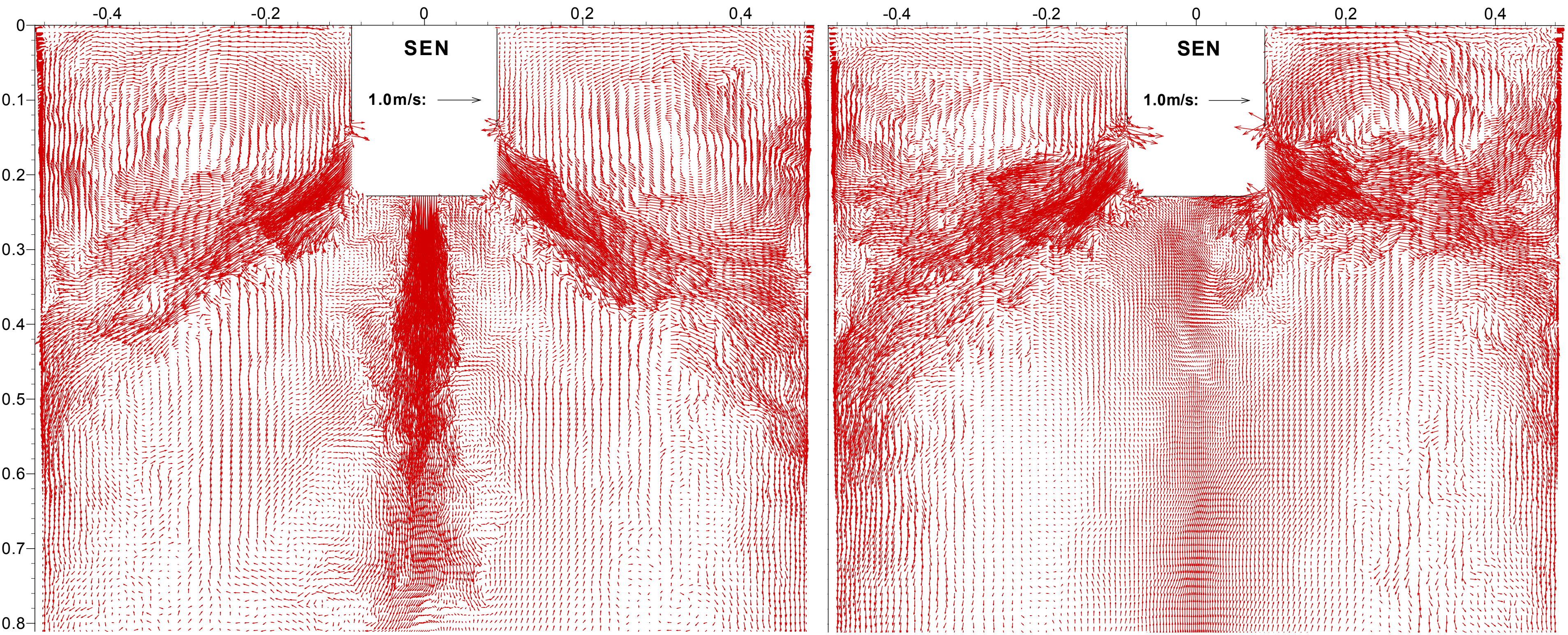

Flow with center nozzle port

(same time instant as right plot)

Flow with center nozzle port blocked

(28.4 s after blocking)

Steel Caster vs. Water Model

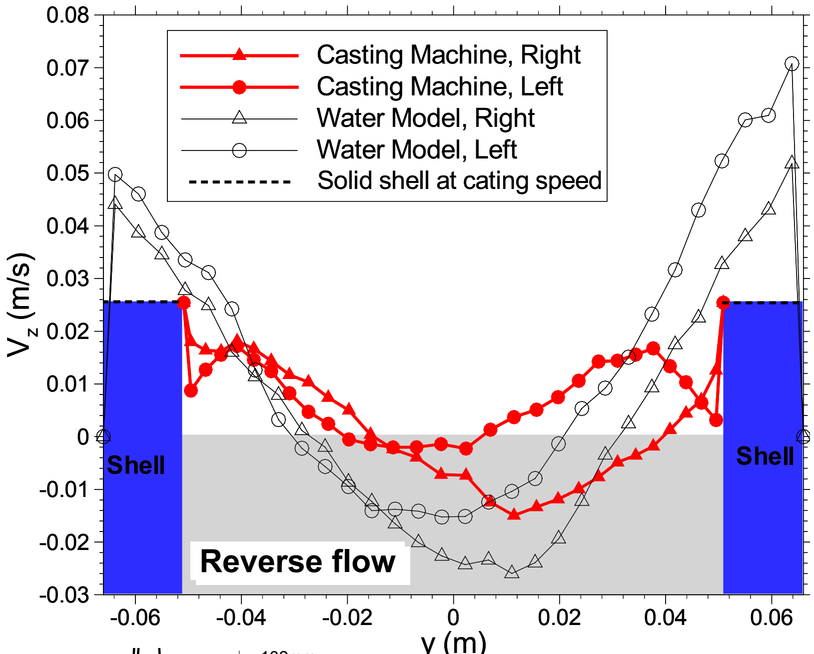

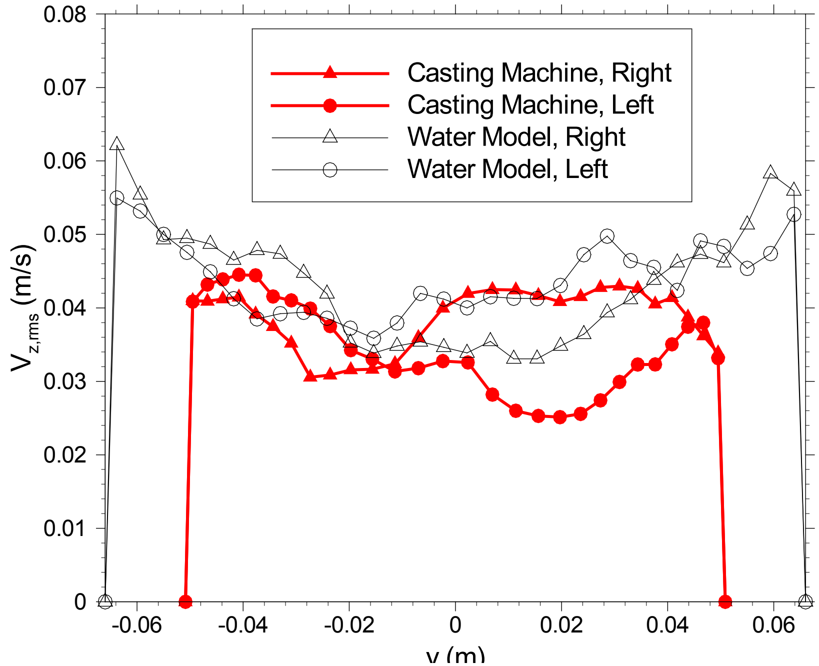

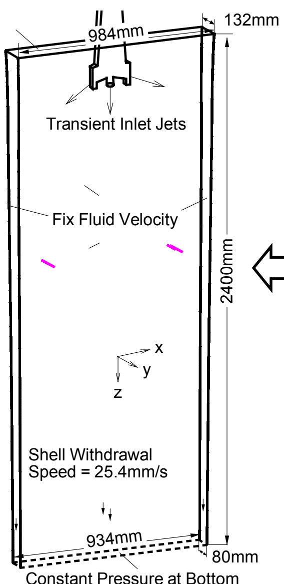

Time-averaged downward velocity (V_z) and its *rms*

Data obtained along horizontal lines 1m below top surface, 164mm from narrow faces.

Top Surface Level Profiles

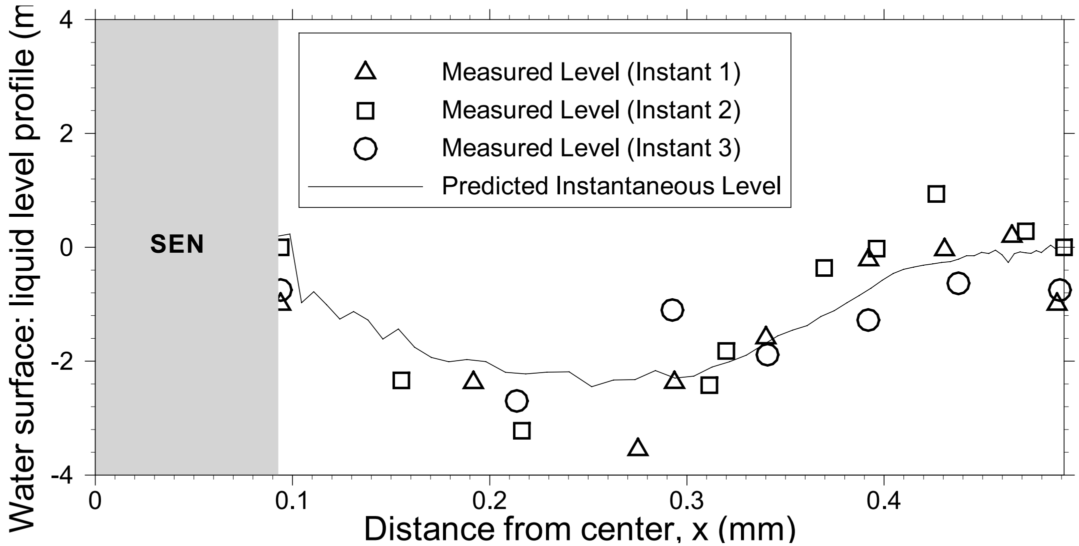

⇦ Water model

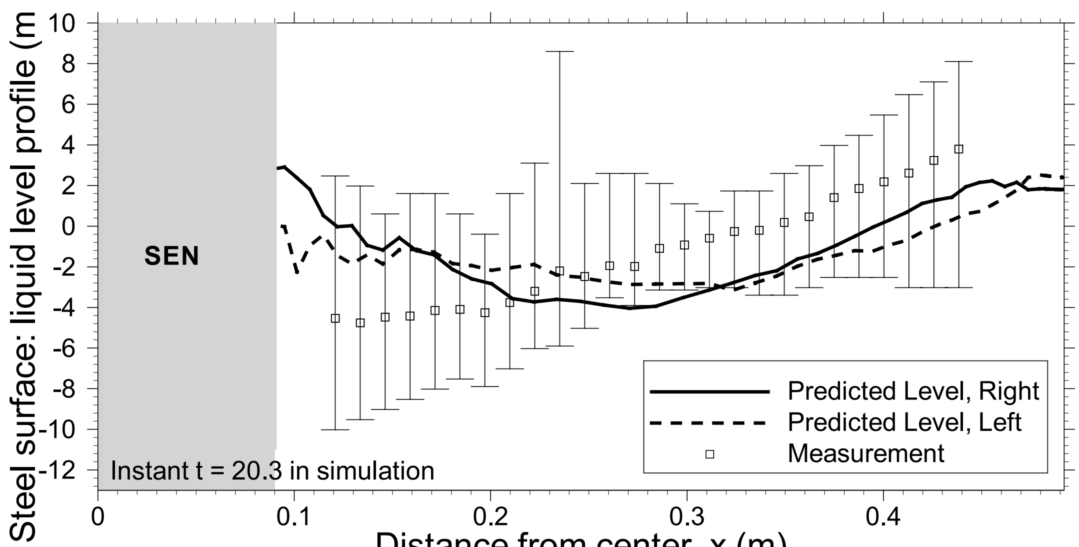

⇦ Steel Caster

Liquid level is calculated from predicted pressure:

$$h = \frac{(p - p_{mean})}{(\rho_{steel} - \rho_{flux})g}$$

Top Surface Velocity Fluctuations

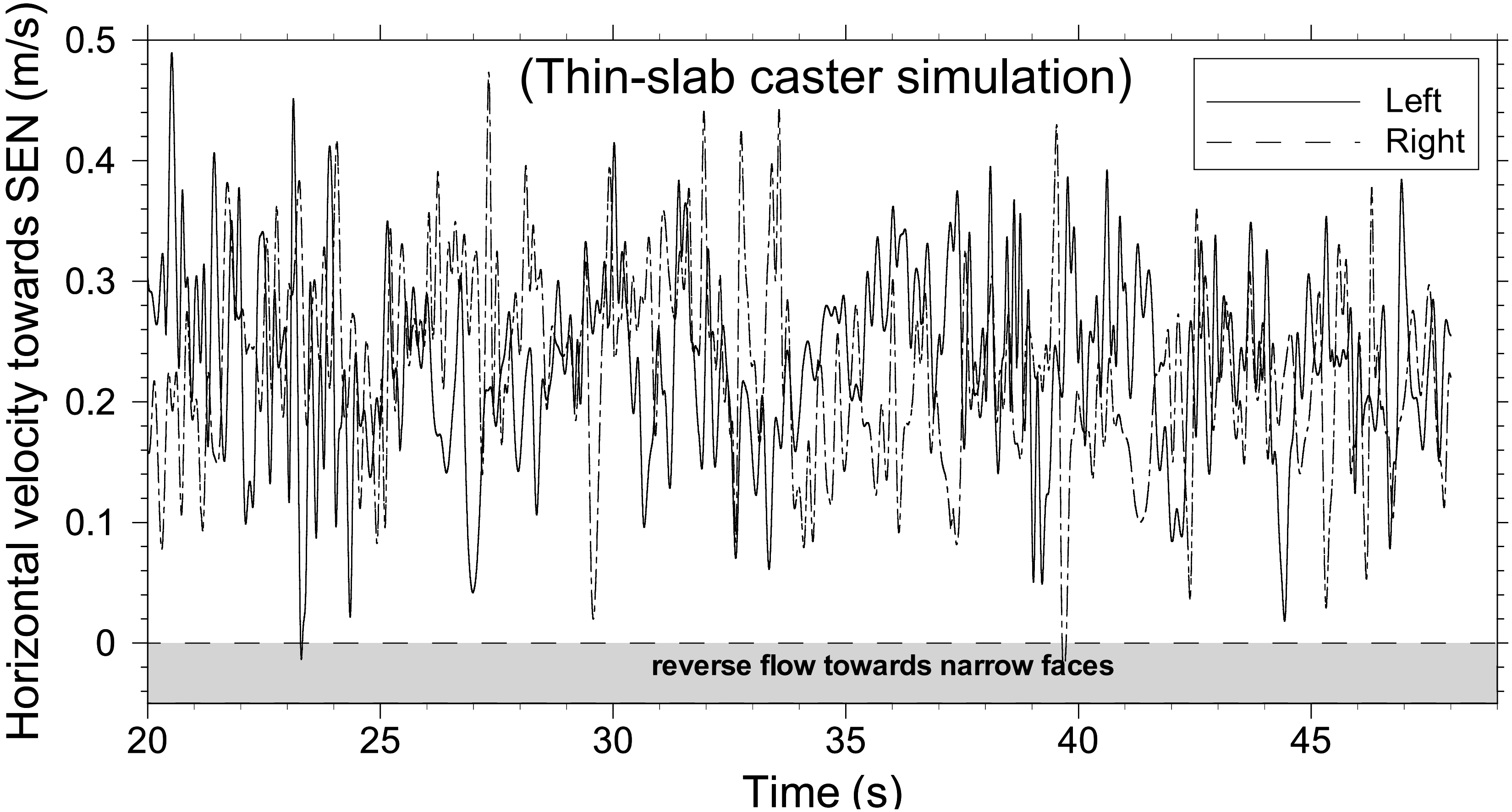

Similar high frequency, large fluctuation components are also observed in thin-slab caster

Frequency distribution of u-velocity fluctuations (from Fourier analysis of LES signals)

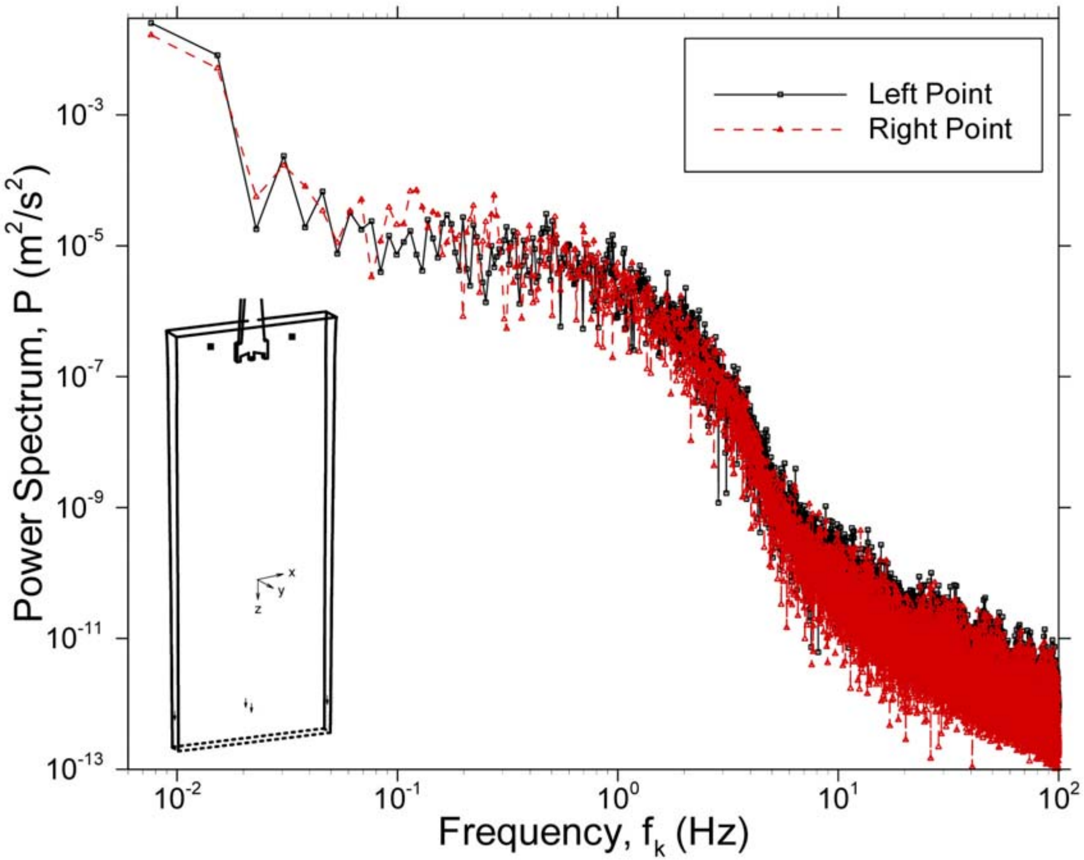

$$P(f_k) = \begin{cases} \dfrac{1}{N^2}\left|C_k\right|^2, & k = 0, \dfrac{N}{2} \\ \dfrac{1}{N^2}\left(\left|C_k\right|^2 + \left|C_{N-k}\right|^2\right), & k = 1, \ldots, \dfrac{N}{2} - 1 \end{cases}$$

where

$$C_k = \sum_{n=0}^{N-1} \mathrm{v}_x\left(t_n\right) e^{\mathbf{i}2\pi f_k t_n}$$

$$f_k = \frac{k}{t_{N-1} - t_0}, \quad k = -\frac{N}{2}, \ldots, \frac{N}{2} - 1$$

A similar behavior of the power spectrum is observed in measurements on a scaled water model Lawson and Davidson (2002).

Transport and Entrapment of Particles in Thin-Slab Steel Caster

Inclusion Pushing/Capture Mechanisms (Review)

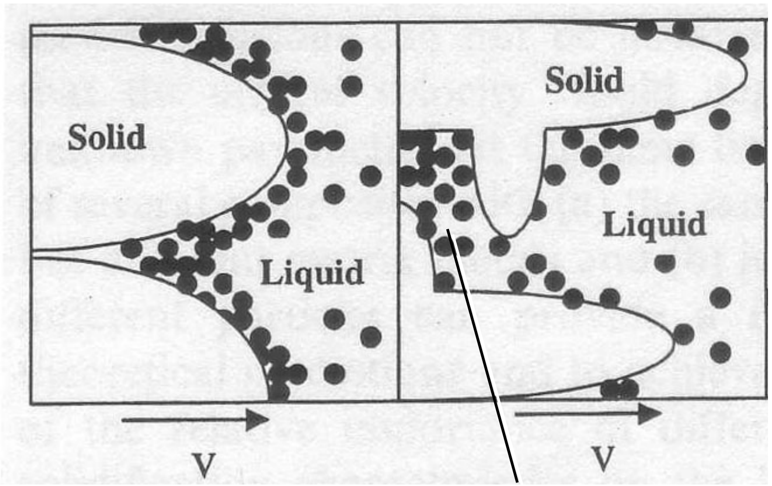

pushing **entrapment**

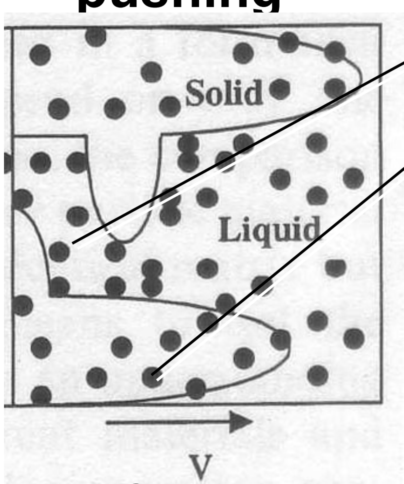

engulfment

In Simulation:
Particle diameter: 10 & 40μm
Particle density: 2700 & 5000Kg/m³

From: G. Wilde, J.H. Perepezko, Experimental Study of Particle Incorporation during Dendritic Solidification, Materials Science & Engineering A283, 2000, p.25-37.

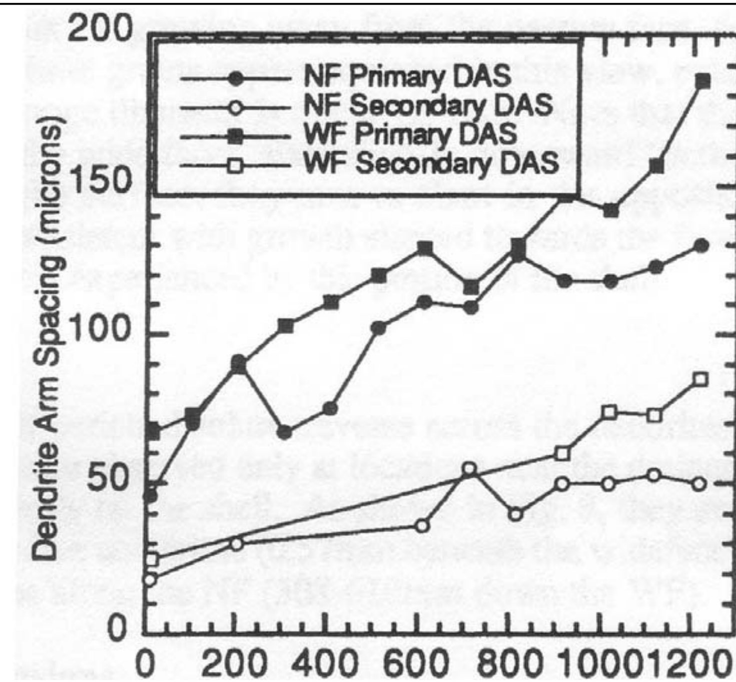

Distance below top meniscus (mm)

From: B.G. Thomas, R. O'Malley and D. Stone, *Measurement of Temperature, Solidification, and Microstructure in a Continuous Cast Thin Slab*, TMS. Warrendale, PA, 1998, pp.1185-1199.

Particle Motion near Stopper Rod

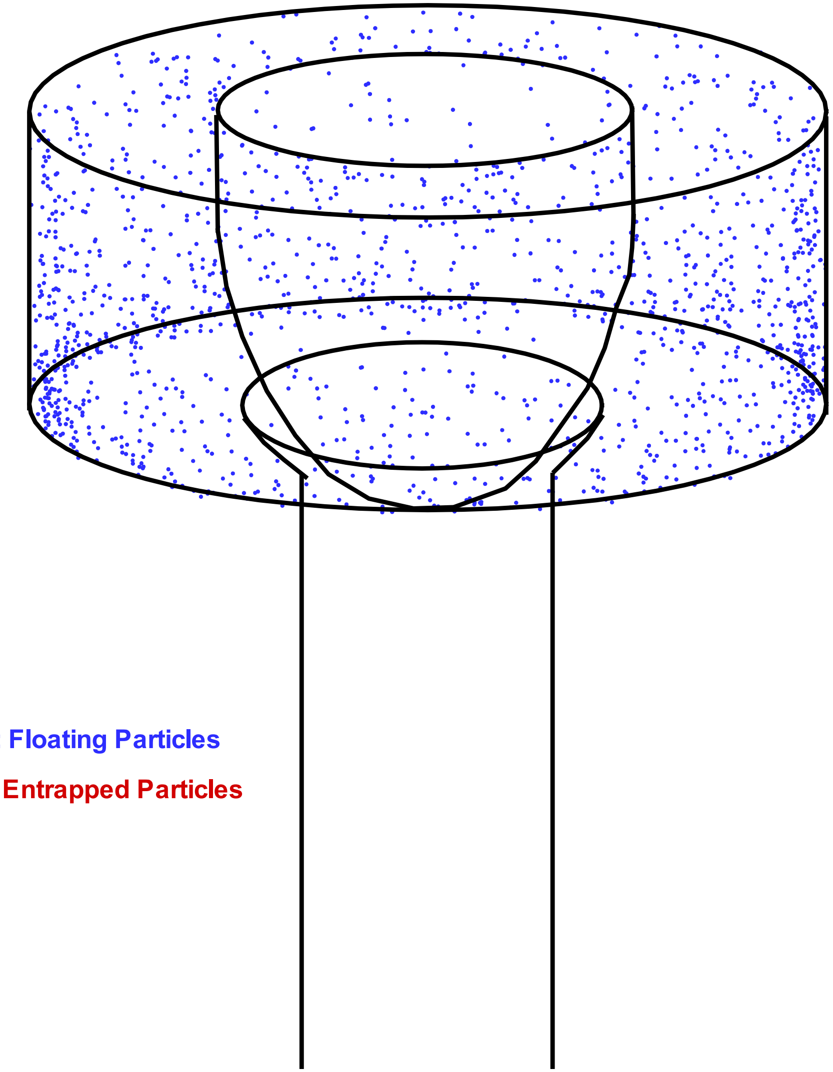

Particles Attached to Nozzle Inner Wall

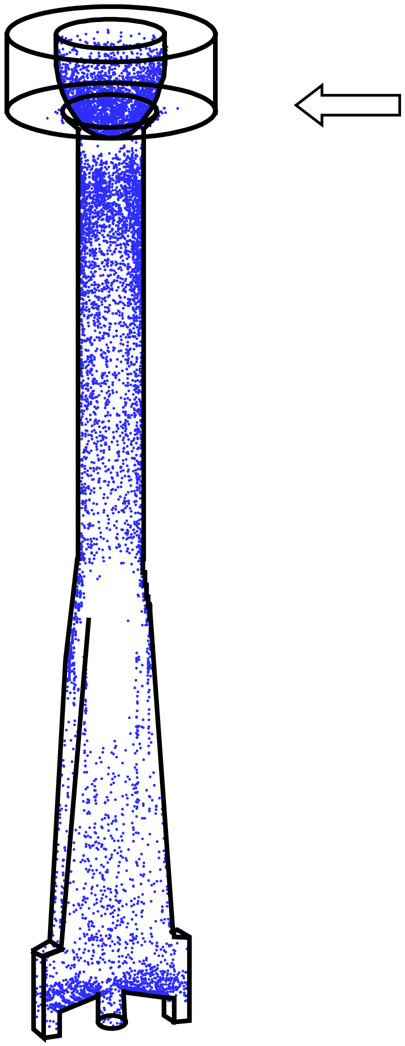

16% of the particles exiting the tundish touched an inner wall of the nozzle and another 10% touched the stopper rod.

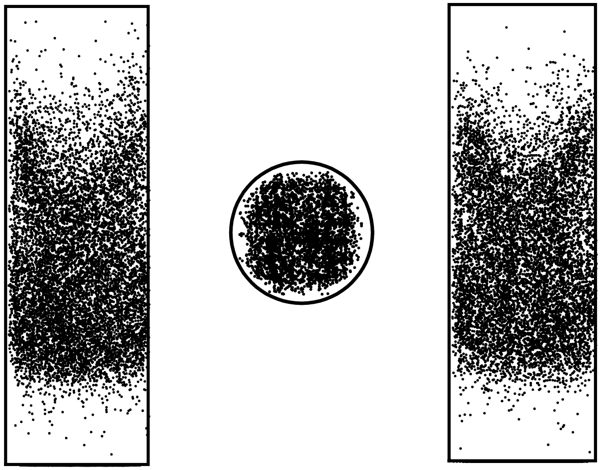

Locations where particles exit nozzle port.

Particle Motion in Steel Caster

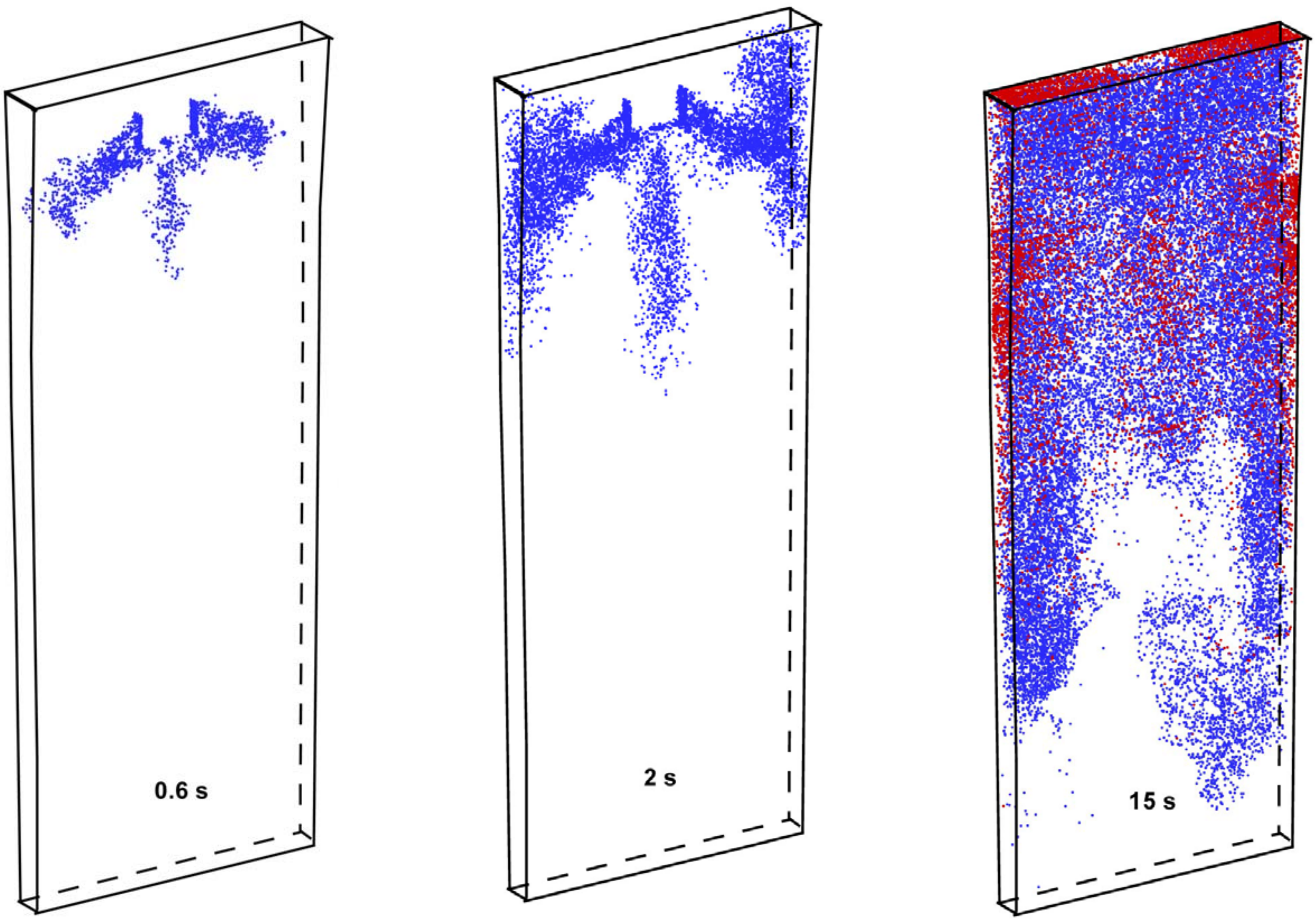

Asymmetrical Inclusion Distribution in Solid Steel (Previous Work)

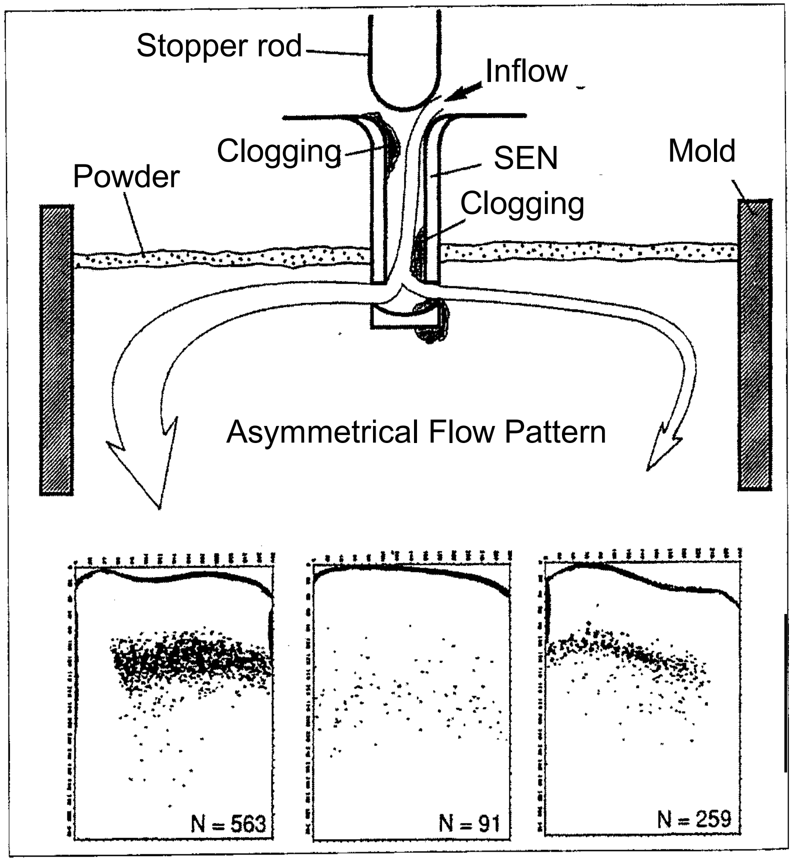

Asymmetrical inclusion capture observed in plants
Suspected Cause: Asymmetrical inlet flow

From: Jacobi, H., H.-J. Ehrenberg, and K. Wuennenberg, *Development of the cleanness of different steels for flat and round products.* Stahl und Eisen, 1998. 118(11): p. 87-95

What Causes Asymmetrical Particle Transport in Simulation?

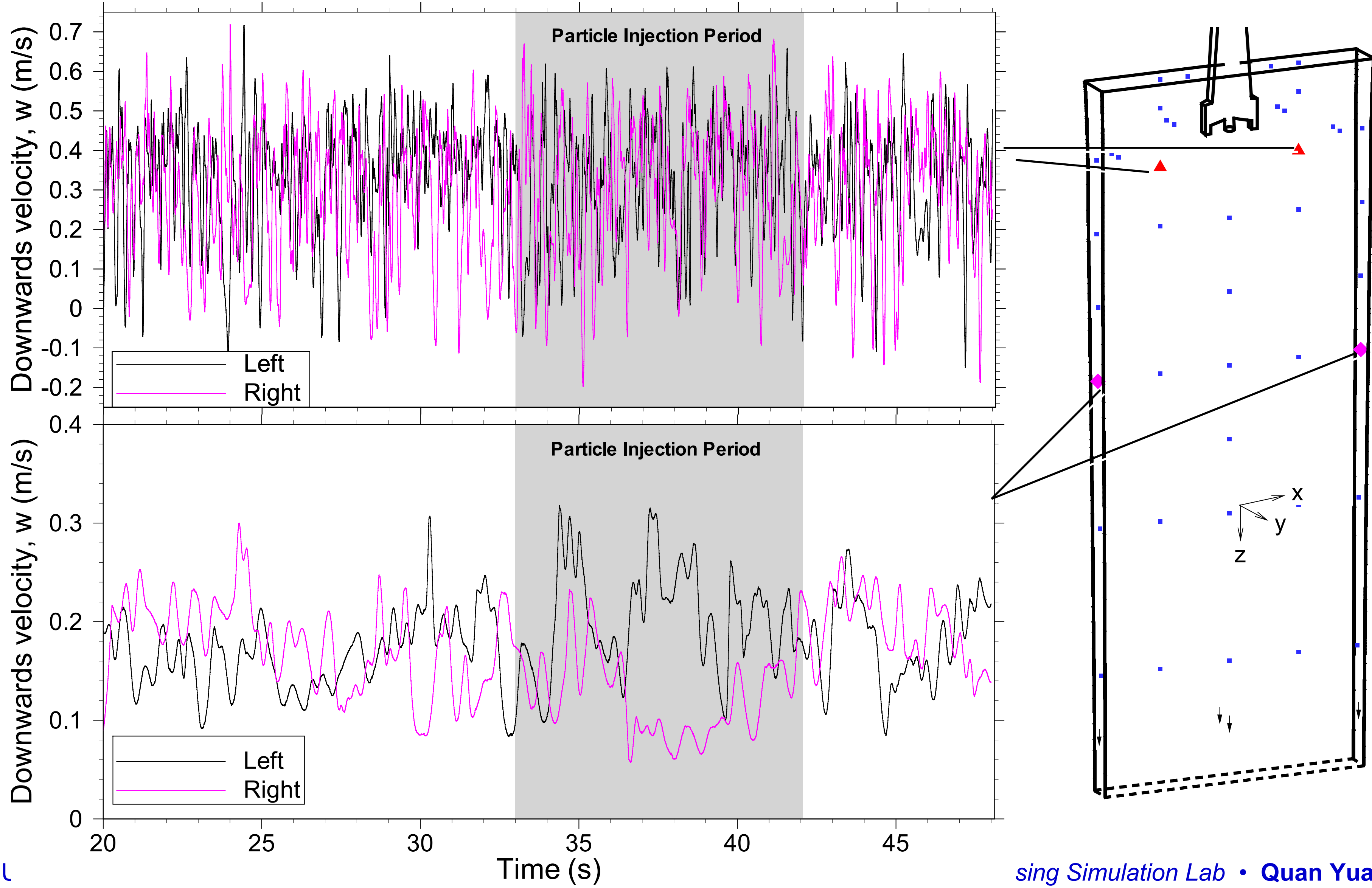

Particle Removal and Entrapment History

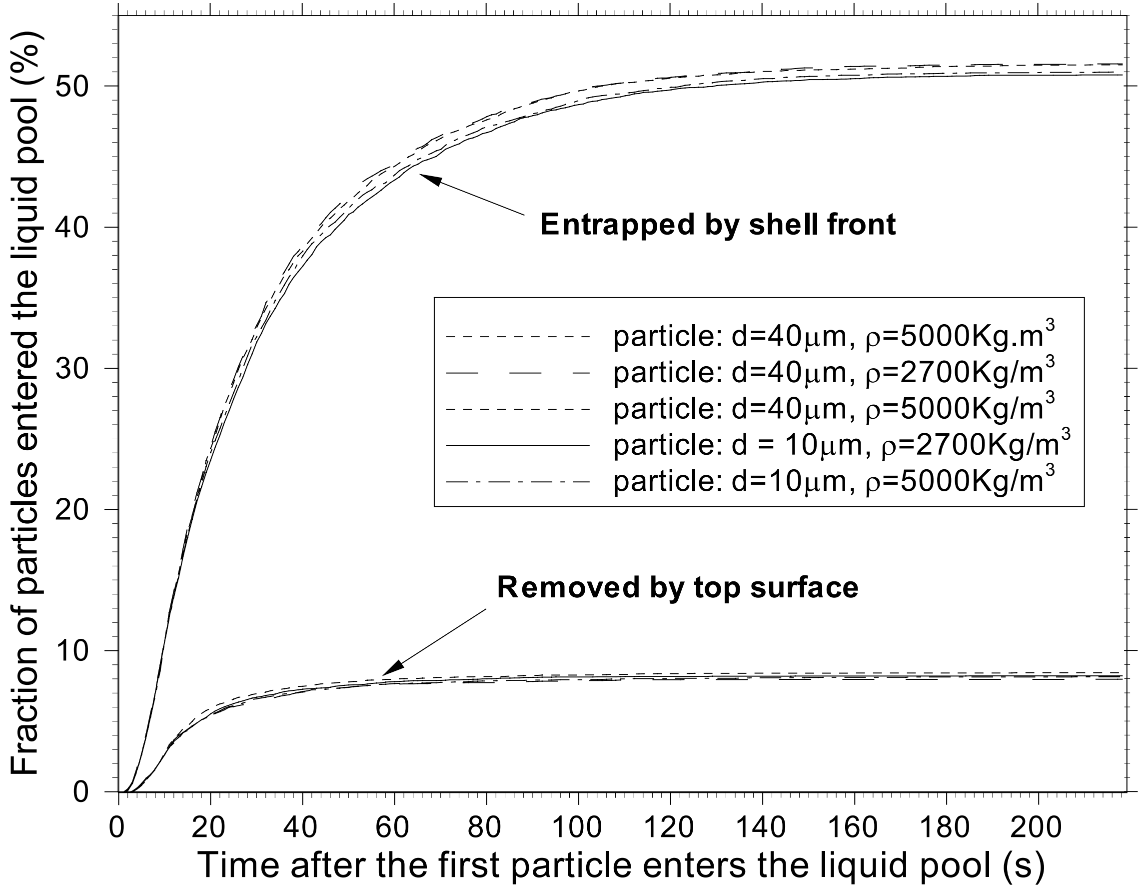

Diameter (μm)	40	10
Density (Kg/m^3)	2700	5000
Entrapment to shell	51.51%	50.79%
Entrapment deeper	32.07%	32.77%
Removal by top surface	8.49%	8.23%
Removal by nozzle wall	7.83%	8.03%

~8% particle removal by top surface

Inclusions Distribution in Solid Slab

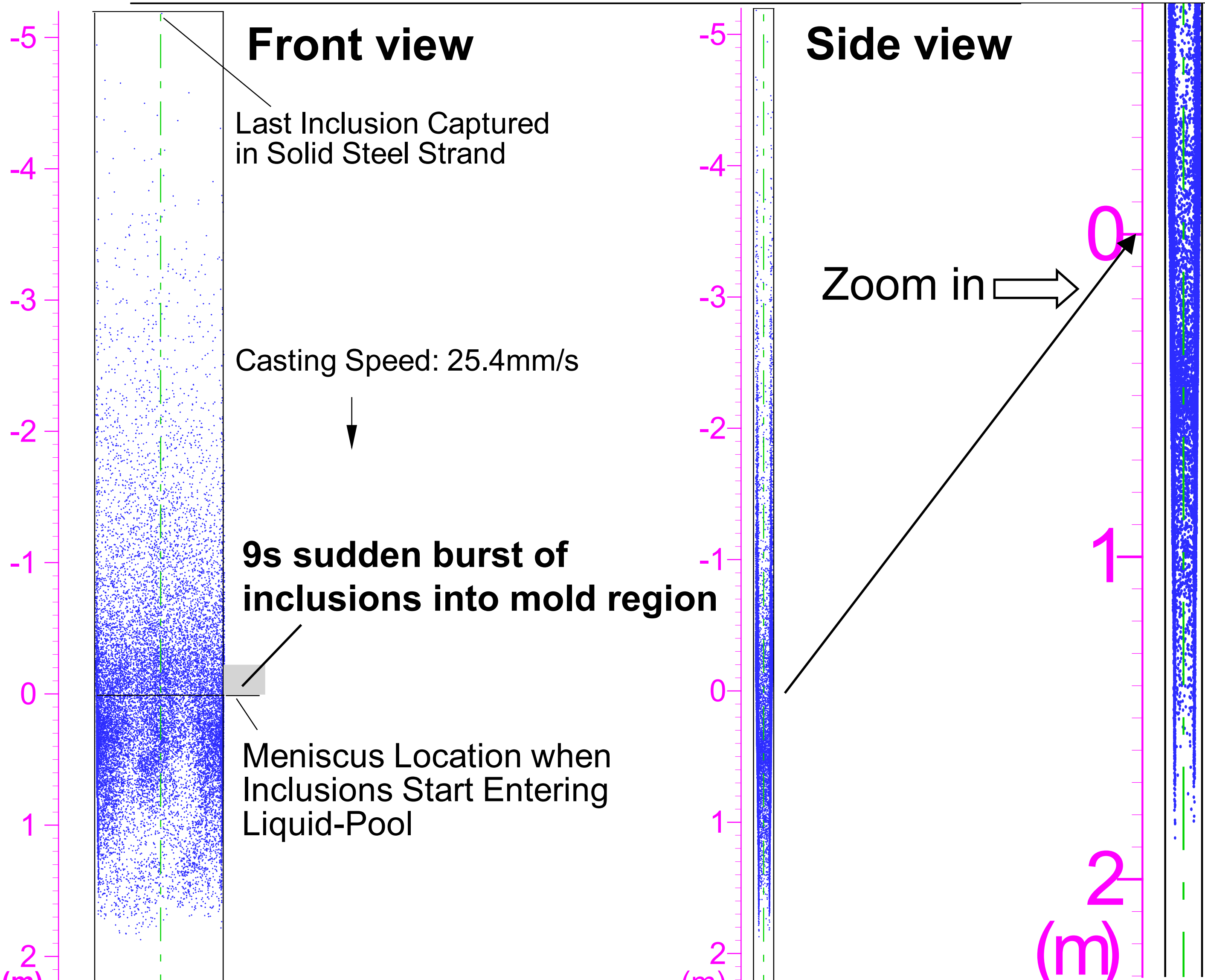

20345 captured particles out of all 40000 particles entered mold.

Inclusion size:

10 and 40 μm

Inclusion density:

2700 and 5000 Kg/m^3

Predicted Total Oxygen

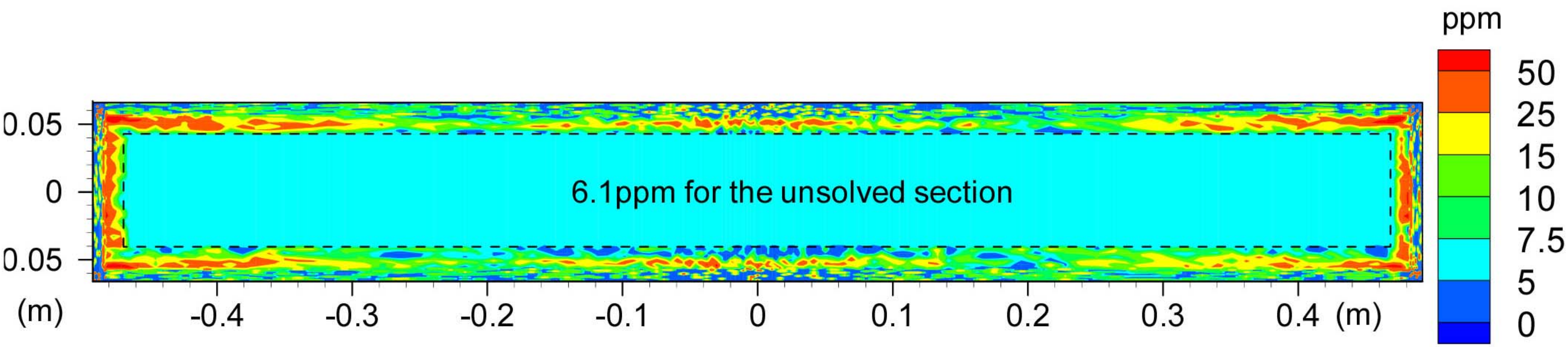

Predicted oxygen concentration in final steel slab

(10ppm oxygen from continuous injection of particles from nozzle ports).

Oxygen concentration is computed by:

$$C_o = \frac{(48/102)\ M_p}{\rho(\Delta x \Delta y \Delta z) + (1 - \rho / \rho_p) M_p}$$

where:

$$M_p = \sum_{i=1}^{N_C} \frac{\pi d_p^3 \rho_p}{6}$$

Conclusions

- LES reproduces time-averaged and *rms* velocities which agree with measurements
- Complex particle trajectories are seen in both the water model and the actual steel caster, showing the important influence of turbulence on particle transport. The simulated particle trajectories as well as the predicted removal fractions are in agreement with water model measurements.
- Water models is generally representative of modeling single-phase flow field in actual steel casters; however, more reverse flow was observed at lower recirculation zone in the water model than in the steel caster
- Flow asymmetry due to turbulence nature causes particle transport asymmetry
- Transport and capture of small particles (d_p<40μm) are similar in the steel caster; removal of smalls particles by top surface in mold region is ~8%
- With a steady oxygen content of 10ppm from inclusions in the molten steel supplied from the nozzle ports, intermittent patches of high oxygen content (50-150ppm) are found concentrated within 10-20mm beneath the slab surface, especially near the corner, and towards the narrow faces.